Wireless Biomedical Sensor Network Reference Design Based on the Intel® Edison Platform

by

Tianyu Lin

B.S., Kansas State University, 2013

A THESIS

submitted in partial fulfillment of the requirements for the degree

MASTER OF SCIENCE

Department of Electrical & Computer Engineering
College of Engineering

KANSAS STATE UNIVERSITY
Manhattan, Kansas

2017

Approved by:

Major Professor
Steve Warren

Copyright

© 2017 Tianyu Lin

Abstract

A reference design for a wearable, wireless biomedical sensor set has been a long-term need for researchers at Kansas State University, driven by the idea that a basic set of sensor components could address the demands of multiple types of human and animal health monitoring scenarios if these components offered even basic reconfigurability. Such a reference design would also be a starting point to assess sensor performance and signal quality in the context of various biomedical research applications.

This thesis describes the development of a set of wireless health monitoring sensors that can be used collectively as a data acquisition platform to provide biomedical research data and to serve as a baseline reference design for new sensor and system development. The host computer, an Intel Edison unit, offers plug-and-play usability and supports both Wi-Fi and Bluetooth wireless connectivity. The reference sensor set that accompanies the Intel Edison single-board computer includes an electrocardiograph, a pulse oximeter, and an accelerometer/gyrometer. All sensors are based on the same physical footprint and connector placement so that the sensors can be stacked to create a collection with a minimal volume and footprint.

The latest hardware version is 3.1. Version 1.0 supported only a pulse oximeter, whereas version 2.0 included an electrocardiograph, pulse oximeter, and respiration belt. In version 3.0, the respiration belt was removed, and accelerometers and gyroscopes were added to the sensor set. Version 3.1 is a refined version of the latter design, where known hardware bugs were remedied. Future work includes the development of new sensors and casing designs that can hold these sensor stacks.

Table of Contents

List of Figures vi
List of Tables viii
Acknowledgements ix
Chapter 1 - Introduction 1
1.1 Motivation 1
1.2 Background 1
Chapter 2 - System-Level Design and Methods 3
2.1 Architectural Requirements 3
2.2 Single-Board Computer and Microcontroller Selection 3
2.3 System Architecture 4
2.4 Sensor Selection 5
Chapter 3 - Sensor Design 6
3.1 Electrocardiograph 6
3.2 Pulse Oximeter 9
3.3 Accelerometer and Gyroscope 13
3.4 Interfaces and System Support Printed Circuit Boards 15
3.4.1 Battery and Serial Port Board 15
3.4.2 Reflection-Mode Pulse Oximetry Sensors 17
3.4.3 Commercial Pulse Oximetry Sensor Adaptor 20
3.4.4 Commercial ECG Lead Adaptor 20
Chapter 4 - Hardware and Manufacturing 21
Chapter 5 - Firmware Development 26
5.1 Software Flow 26
5.2 Simplified Preconfigured Program 27
Chapter 6 - Results and Analysis 29
6.1 Electrocardiograph 29
6.2 Pulse Oximeter 32
6.3 Accelerometer and Gyroscope 36
6.4 Power Consumption 38

6.5 Sampling Rate Variation 39
Chapter 7 - Conclusion 40
Chapter 8 - References 42
Appendix A - Hardware Schematics 44
Electrocardiograph 44
Pulse Oximeter 46
Accelerometer and Gyroscope 48
Battery and Serial Port Board 50
Appendix B - Hardware PCBs 51
Electrocardiograph 51
Pulse Oximeter 52
Accelerometer and Gyroscope 54
Battery and Serial Port Board 55
Appendix C - Hardware Parts Lists 57
Electrocardiograph 57
Pulse Oximeter 58
Accelerometer and Gyroscope 59
Battery and Serial Port Board 60

List of Figures

Figure 1. ADAS1000 5-electrode ECG analog front end. 7
Figure 2. ADP151AUJZ power supply. 8
Figure 3. AFE4490 integrated analog front end for a pulse oximeter. 11
Figure 4. TXB0104 4-Bit bi-directional voltage-level translator. 12
Figure 5. LT3467A DC/DC boost converter. 12
Figure 6. LT3029 dual low-noise linear regulator. 13
Figure 7. LSM9DS0 accelerometer and gyroscope sensor. 14
Figure 8. ADP151AUJZ power supply. 14
Figure 9. MCP73831 li-polymer charge management controller. 15
Figure 10. FT230X USB to basic UART IC. 16
Figure 11. Switches and LED indicators. 17
Figure 12. Schematic for a reflection-mode pulse oximetry sensor (quad photodiodes). 18
Figure 13. PCB layout for a reflection-mode pulse oximetry sensor (quad photodiodes). 18
Figure 14. Schematic for a reflection-mode pulse oximetry sensor (single photodiode). 19
Figure 15. PCB layout for a reflection-mode pulse oximetry sensor (single photodiode). 19
Figure 16. Intel Edison physical dimensions. 21
Figure 17. Intel Edison package front and back. 22
Figure 18. ECG sensor PCB front and back. 22
Figure 19. Pulse oximeter sensor PCB front and back. 23
Figure 20. Accelerometer and gyroscope sensor PCB front and back. 23
Figure 21. Battery and serial port PCB front and back. 24
Figure 22. Single photodiode and quad photodiode sensor probes. 25
Figure 23. Side view of a one-sensor stack. 25
Figure 24. Software flow diagram. 26
Figure 25. Simplified preconfigured program flowchart. 28
Figure 26. Three-lead ECG sample data. 29
Figure 27. Three-channel ECG zoomed-in plots. 30
Figure 28. Single-sided amplitude spectrum for the LL-LA channel. 31

Figure 29. Zoomed-in, single-sided amplitude spectrum for the LL-LA channel. 31
Figure 30. PPGS obtained with a commercial finger probe. 32
Figure 31. FFT-based amplitude spectrum for a red PPG obtained with the commercial finger probe. 33
Figure 32. Zoomed-in amplitude spectrum for the infrared PPG (commercial finger probe). 34
Figure 33. PPG plots for the transmissive commercial finger probe, the reflective quad-photodiode probe, and the single-photodiode probes. 35
Figure 34. Amplitude spectra for the transmissive commercial finger probe, the reflective quad-photodiode probe, and the single-photodiode probes. 36
Figure 35. Accelerometer and gyroscope signals. 37
Figure 36. Histogram of sampling intervals. 39
Figure 37. ECG schematics – page 1. 44
Figure 38. ECG schematics – page 2. 45
Figure 39. Pulse oximeter schematics – page 1. 46
Figure 40. Pulse oximeter schematics – page 2. 47
Figure 41. Pulse oximeter schematics – page 3. 47
Figure 42. Accelerometer and gyroscope schematics – page 1. 48
Figure 43. Accelerometer and gyroscope schematics – page 2. 49
Figure 44. Battery and serial port schematics – page 1. 50
Figure 45. Battery and serial port schematics – page 2. 50
Figure 46. ECG PCB layer top and bottom. 51
Figure 47. ECG PCB layer power and ground. 51
Figure 48. Pulse Oximetry PCB Layer Top and Bottom 52
Figure 49. Pulse oximeter PCB layer power and ground 53
Figure 50. Pulse oximeter PCB assembly top and bottom 53
Figure 51. Accelerometer and gyroscope PCB layer top and bottom. 54
Figure 52. Accelerometer and gyroscope PCB layer power and ground. 54
Figure 53. Accelerometer and gyroscope PCB assembly top and bottom. 55
Figure 54. Battery and serial Pprt PCB layer top and bottom. 55
Figure 55. Battery and serial port PCB layer power and ground. 56
Figure 56 Battery and serial port PCB assembly top and bottom. 56

List of Tables

Table 1. Single-board computer options. 4
Table 2. Power consumption..... 38
Table 3 ECG Sensor Parts List 57
Table 4 Pulse Oximetry (SpO2) Sensor Parts List..... 58
Table 5 Accelerometer and Gyroscope Sensor Parts List..... 59
Table 6 Battery and Serial Port Board Parts List..... 60

Acknowledgements

This material is based upon work supported by the National Science Foundation (NSF) General & Age-Related Disabilities Engineering (GARDE) Program under grants CBET–1067740 and UNS–1512564. Opinions, findings, conclusions, or recommendations expressed in this material are those of the author(s) and do not necessarily reflect the views of the NSF.

Chapter 1 - Introduction

1.1 Motivation

Demand for reliable wireless biomedical sensors for research and education has been steadily increasing in recent years, in part due to emerging wearable and cell-phone-based applications, spurred by new developments in support of the Internet of Things. The objective of this research was to design and build a set of biomedical sensors that could be easily joined together to create a small, wearable, wireless, multi-vital-sign monitoring platform that could then be easily reconfigured to support various human and animal health monitoring applications. This design would serve as a reference design for future customized systems. The biomedical sensor set, controlled with an Intel® Edison single-board computer, includes an electrocardiograph, a pulse oximeter, and an accelerometer/gyrometer (gyroscope) pair. These sensors interface with the Intel Edison microcontroller board via a 70-pin connector that promotes easy connections and disconnections. The device architecture allows multiple sensors to be stacked onto one Intel Edison board. Data are streamed through a USB port or wirelessly over either a Wi-Fi or Bluetooth connection.

1.2 Background

Researchers at Kansas State University have conducted several wireless biomedical sensor projects in recent years that resulted in innovative designs. In 2005, Jianchu Yao designed standards-based medical components and a plug-and-play home health monitoring system. This work promoted Bluetooth-based plug-and-play biomedical sensors for health monitoring and demonstrated the implementation of the IEEE 1073 (now IEEE 11073) standard on wearable, battery operated devices that utilized no operating system [1]. In 2010, Kejia Li investigated

wireless reflectance pulse oximeters and photoplethysmographic signal processing – efforts that included the design of two versions of a reflectance pulse oximeter based on a Jennic JN5139 ZigBee wireless module [2]. In addition, in 2012, Kejia Li studied the application of custom biomedical sensors in wireless body area networks and medical device integration frameworks. This “GumPack” system utilized a GumStix Overo single-board computer and demonstrated wireless connectivity (Wi-Fi, Bluetooth, and ZigBee). Biomedical sensors included a pulse oximeter, a single-channel ECG, and an accelerometer/gyroscope [3]. In 2014, Xiongjie Dong utilized Kejia Li’s ZigBee-based reference design to develop a ZigBee-based wireless biomedical sensor network as a precursor to an in-suit system for monitoring astronaut state of health, resulting in the development of two-channel ECG sensors, a respiration rate belt, an accelerometer/gyrometer, and an electromyograph [4].

Chapter 2 - System-Level Design and Methods

2.1 Architectural Requirements

An architecture for a wearable, wireless embedded device must be user-friendly, reliable, and cost-effective, and the microcontroller must be selected to ensure that the sensor set has a reasonably long life cycle, e.g., six to ten years. Its physical dimensions must be suitable for mounting the device on, e.g., the wrist, and acquired data must be able to stream to a personal computer or be saved locally. Battery life should be at least two hours to avoid user frustration.

2.2 Single-Board Computer and Microcontroller Selection

A number of single-board computers and their respective microcontrollers have recently emerged for wearable, wireless health monitoring applications. The ideal microcontroller board for this effort had to offer small physical dimensions, wireless connectivity, and a solder-free interface. One suitable candidate from the unit [5]. Another alternative, the Raspberry Pi 3, is the third generation in a successful Raspberry Pi family [6]. The Intel Edison is strongly promoted by the world's foremost integrated circuit manufacturer [7], and the RFduino Dip is provided by a startup company and offers value in a small footprint [8]. Table 1 compares physical dimensions, wireless functionality, and connector heights for these single-board computer options. The Intel Edison unit was determined to be the most suitable host for this reference architecture.

Table 1. Single-board computer options.

	Length (mm)	Width (mm)	Height (mm)	Wi-Fi	BT	Solder-free interface	Additional connector height for each sensor (mm)
Arduino MKR1000	61.5	25	18	Yes	No	Yes	10
Raspberry Pi 3	85	56	17	Yes	Yes	Yes	10
Intel Edison	33	25	4	Yes	Yes	Yes	3
RFduino DIP	29	23	18	No	Yes	Yes	10

Selection of the ideal microcontroller board for this research also considered the software integrated development environment (IDE), the product life cycle, customer support, retailers, price, and supply stability. Regarding software development, the Intel Edison unit supports C and Python within the Eclipse IDE, consistent with Arduino offerings. In terms of life cycle, customer support, and supply stability, the Intel Edison product has support from the world's largest integrated circuit manufacturer, Intel. The Intel Edison unit is available at most major electronics retailers, and SparkFun has offered evaluation board support for the Intel Edison. The retail price of an Intel Edison unit is $59.99.

2.3 System Architecture

The system architecture for this reference design is configurable and extendable. The physical biomedical sensor stack is comprised of one or more sensor boards and one Intel Edison microcontroller unit. The design has progressed through versions 1.0, 2.0, 3.0 and 3.1. In versions 1.0 and 2.0, each sensor board had a battery management circuit, a lithium polymer battery, a micro USB charging port, and a power switch. A simple baseline setup contained one sensor board stacked with an Intel Edison unit. A multiple-sensor stack based on this approach, however, was disadvantageous due to the presence of multiple batteries: additional batteries required for the sensor(s) in the intermediate layers needed to be unsoldered. In addition,

multiple micro USB charging ports and power switches could remain unused in the intermediate layers, adding unintended thickness to the overall device.

Changes to the system in version 3.0 allowed optimization of the sensor stack and new functionality. For example, the battery management circuit, lithium polymer battery, micro USB charging port, and power switch were separated from the sensor boards as a stand-alone system-support board (known as the battery and serial port board). This board also contains a USB COM (communication) port to UART (universal asynchronous receiver/transmitter), multiple LED indicators, and multiple slide switches.

2.4 Sensor Selection

Biomedical sensors to be stacked with an Intel Edison unit must share the same footprint. Initial candidates were derived from previous designs from the Kansas State University Electrical & Computer Engineering department: a pulse oximeter from Kejia Li in 2010 [2], an accelerometer and gyroscope from Devon Krenzel in 2012 [9], and a respiration belt and electrocardiograph from Xiongjie Dong in 2014 [4]. The respiration belt was removed after hardware version 2.0 due to the lack of a built-in digital counter for frequency calculation.

Chapter 3 - Sensor Design

3.1 Electrocardiograph

An electrocardiograph (ECG) utilizes at least one pair of external electrodes placed on the skin to capture the electrical activity of the heart versus time. ECG signal acquisition is challenging because the native signal amplitude is approximately 0.5 mV, with an offset of ~300 mV due to electrode voltage offsets (differences in half-cell potentials), respiration, body movement, etc. In addition, an ECG can detect 50 or 60 Hz noise from power lines that may provide common mode signals to the front-end electronics. This power line noise can overwhelm the ECG signal itself, requiring noise filtering in order to acquire a clean ECG signal.

Therefore, analog front-end processing is essential to the ECG system since the system must distinguish between noise and the desired ECG signal with a small amplitude (~0.5 mV). A front-end processing circuit typically utilizes an instrumentation amplifier with a high common-mode rejection ratio as well as a second amplifier stage and filter stage. These stages require additional board space and power, which are already in limited supply, driving the need to discover a compact and efficient solution.

The Analog Devices ADAS1000 [10] is an analog front-end system that can measure an ECG signal, respiration, pacing artifacts, and lead on/off status. This chip-based system is compact (~ 9 mm by 9 mm) and requires very few external elements. Its low-power mode is ideal for this research application. The ADS1000 has a serial interface that is SPI- /QSPI™-/DSP-compatible within a 64-lead LFCSP package. The ECG channel consists of a differential pre-amplifier with programmable gain and low noise, a lowpass filter with a programmable bandwidth, a differential amplifier buffer with a programmable gain, and a 14-bit SAR ADC at a sampling rate of 2.048 MHz. After internal digital filtering, the ADAS1000 ADC resamples the

signal at 24-bits and a 2 kHz sampling rate, resulting in a signal with 19 usable bits [10]. The ADAS1000 circuitry (chip and external elements) are illustrated in Figure 1.

ECG sensor development for the Intel Edison stack began in version 2.0. In version 3.0, the ECG printed circuit board utilized most of the components from the version 2.0 design, including an ADAS1000 ECG analog front end and an Analog Devices ADP151AUJZ-3.3 voltage regulator – see Figure 2 [11]. However, the battery charging circuit, power switch, and ADP151AUJZ-1.8 V regulator were eliminated. As noted earlier, the battery charging circuit and power switch were moved to a battery and serial port board, and the 1.8 V voltage regulator was replaced by the Intel Edison 1.8 V regulated output.

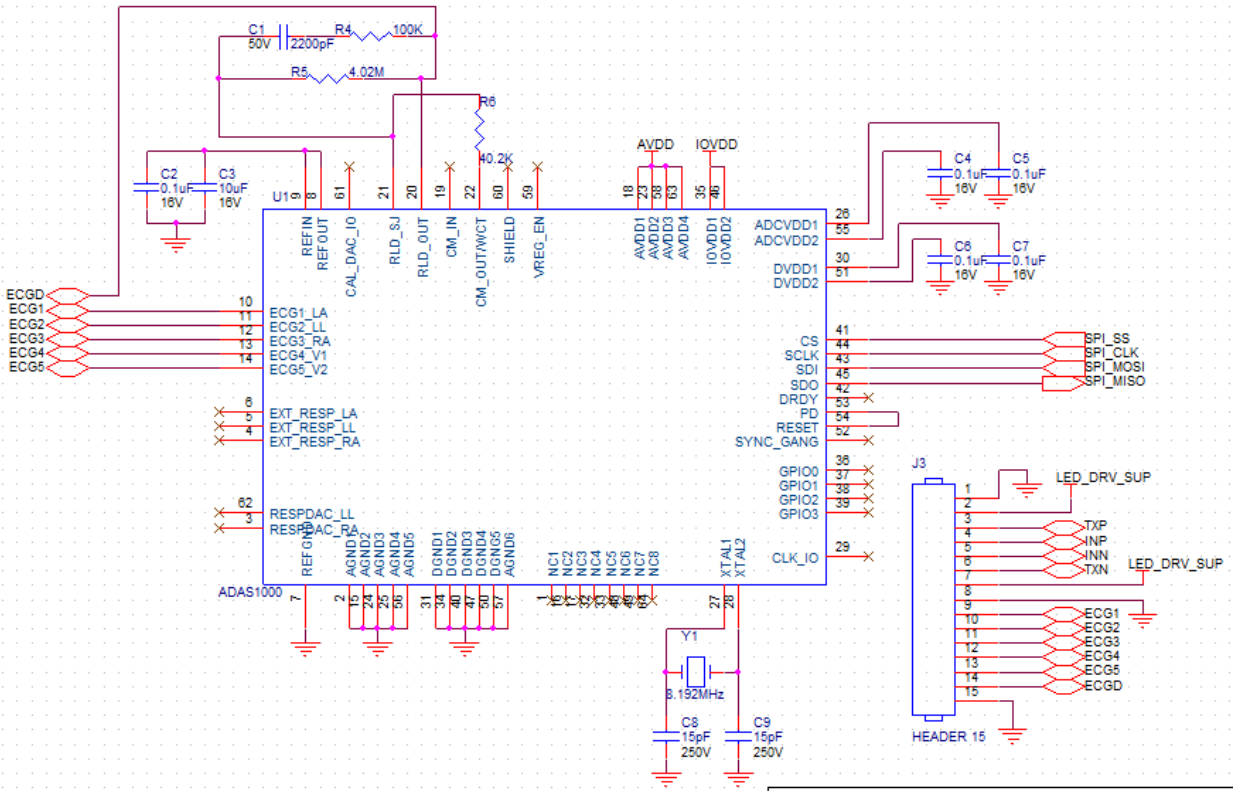

Figure 1. ADAS1000 5-electrode ECG analog front end.

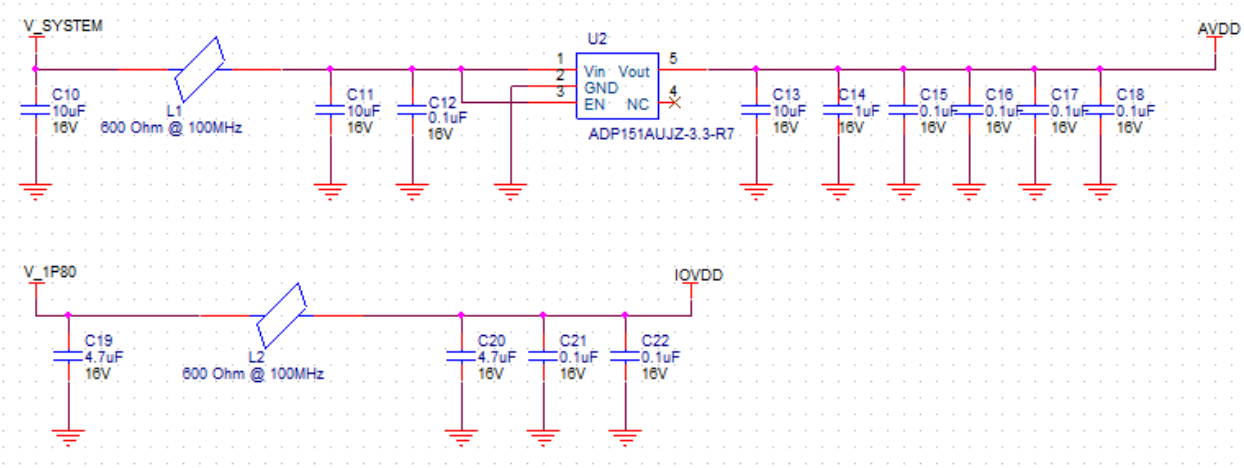

Figure 2. ADP151AUJZ power supply.

The ADAS1000 is a full-featured, 5-channel ECG that includes respiration and pace detection. It offers an IOVDD (input and output V_{DD}) support voltage ranging from 1.65 V to 3.6 V, which corresponds to the Intel Edison digital logic level of 1.8 V. The AVDD (analog V_{DD}) of the ADAS1000 must be 3.3 V ± 5%, but the lithium polymer battery output varies from 3.7 V to 4.3 V, which is out of range. A previous study used an ADP151AUJZ-3.3 CMOS linear regulator to generate a stable 3.3 V source. The ADP151AUJZ-3.3 features ultra-low noise at 9 µV RMS and a maximum output current of 200 mA [11]. Because the IOVDD is not sensitive to noise and draws very little current, using 1.8V from the Intel Edison is a reasonable solution.

In addition to advantageous features such as filters, pacemaker detection, AC/DC lead-off detection, thoracic impedance measurement, and pacing artifact detection, the ADAS1000 offers a small-sized, ultra-low-power solution for measuring ECG signals. Although some features were not applied in the current design, they could be employed in a future application. Extra components or revised design schematics are unnecessary if the designed system needs one of these functions.

3.2 Pulse Oximeter

Photo-plethysmography, a light-based technique that relies on the generation of photo-plethysmograms (PPGs) [2], is commonly used to non-invasively estimate blood volume changes in the microvasculature in peripheral body locations. Compared to other types of plethysmography (e.g., impedance or strain gauge), this optical technique is straightforward to set up and use. PPG systems, which typically employ infrared/red LEDs and photodetectors, operate in two modes: transmission and reflectance.

In the transmission mode, light is transmitted through the tissue and then detected by a photodiode opposite the LED source; in reflectance mode, the photodiode detects light reflected from the tissue. Although the transmission mode can obtain a signal with a relatively good signal-to-noise ratio, the sensor must be positioned on the body in a location where transmitted light can be readily detected (e.g., fingertip, cheek, or earlobe). Unfortunately, however, the fingertip sensor can interfere with daily activities.

Reflectance mode sensors can reduce problems associated with sensor placement by allowing utilization of additional measurement sites (i.e., wrist, earlobe, or superior auricular region). However, a reflectance mode signal can be more severely affected by motion artifacts and pressure disturbances. Signal processing can be employed to reduce, or compensate for, motion artifacts, as discussed in later chapters. The custom design in this study employed a means to accommodate both reflectance-mode and transmission-mode PPG sensors.

Pulse oximeter sensor development began with the sensor set found in version 1.0. The sensor architecture in versions 1.0 and 2.0 was similar to Kejia Li's design, which used three DAC channels to drive the red LED, the infrared LED, and the DC removal feedback circuitry; two ADC channels were used to read raw signals and amplified signals. The ADC and DAC IC

must complete the following sequence for each set of red and infrared samples: turn on the red LED, read the raw red PPG sample, feed the DC portion of the red sample back to the gain stage, read the amplified red sample, turn off the red LED, turn on the IR LED, read the raw IR PPG sample, feed the DC portion of the IR sample back to the gain stage, read the amplified IR sample, and turn off the IR LED. Each set of samples requires ten commands over the serial interface. In version 1.0, an I^2C interface was used between the Intel Edison and the AD5593R ADC/DAC, and the maximum sampling rate achieved was 100 Hz per channel. In version 2.0, an SPI interface was used between the Intel Edison and the AD5592R, and the maximum sampling rate achieved was 200 Hz per channel. However, because the SPI interface was shared with the ECG sensor, timing accuracy and bandwidth were not guaranteed. Therefore, in version 3.0, the design was changed to utilize a Texas Instruments AFE4490 [12] integrated analog front end for pulse oximeters, allowing the timing to be set up during initialization and requiring only one or two commands for each set of samples.

The Texas Instruments AFE4490 integrated front-end module was also advantageous given the limited on-board space and low-power requirement. The AFE4490 consists of a low-noise receive channel, an LED transmit section, and diagnostics for sensor and LED fault detection. It also has a highly configurable timing controller that allows complete control of the device's timing characteristics. The AFE4490, which can be interfaced with an SPI bus, also offers small-sized and ultra-low-power front-end electronics for PPG acquisition. The schematic for the AFE4490 circuitry and external elements is depicted in Figure 3.

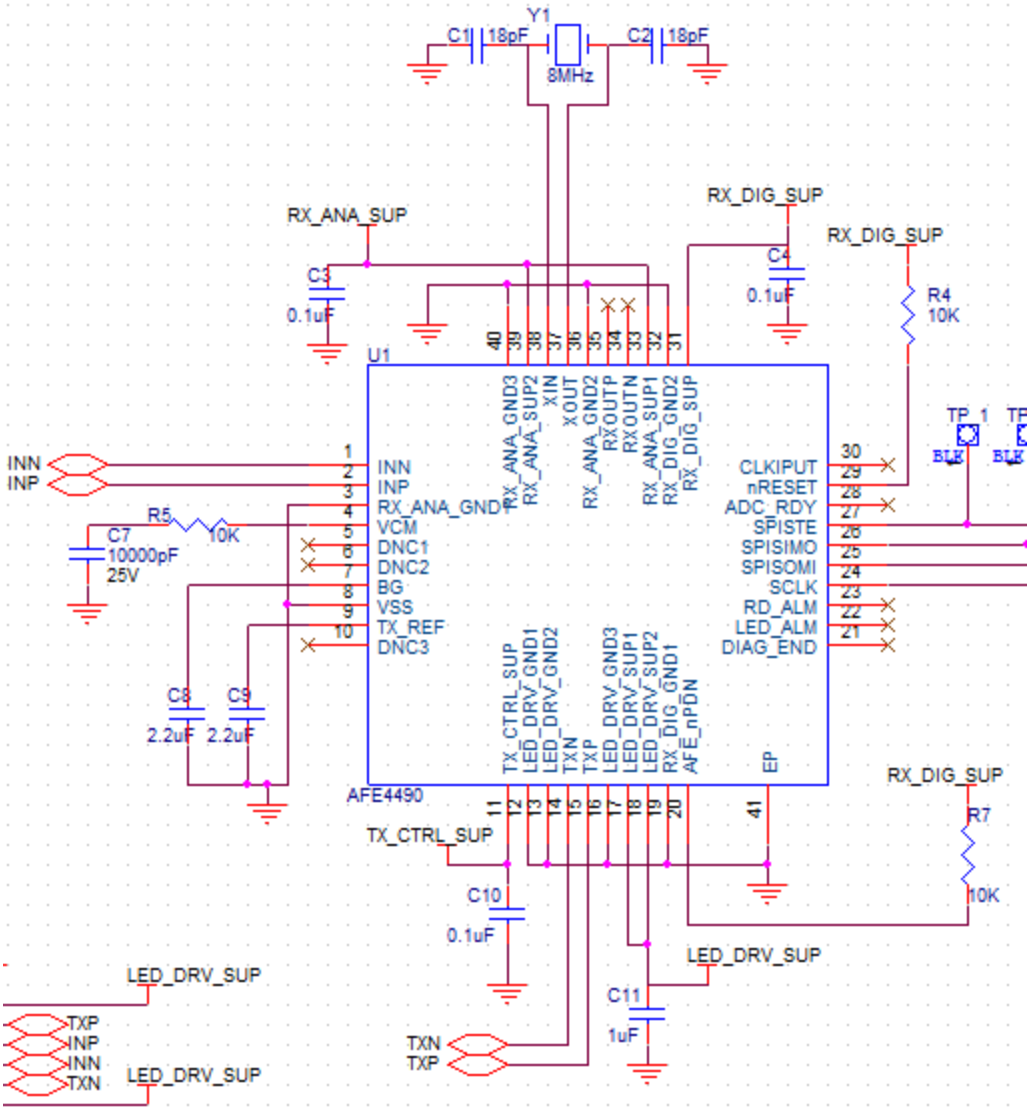

Figure 3. AFE4490 integrated analog front end for a pulse oximeter.

Because the digital IO on the AFE4490 uses 3.3V logic, which is incompatible with the Intel Edison 1.8V logic, a voltage level translator was required, as depicted in Figure 4.

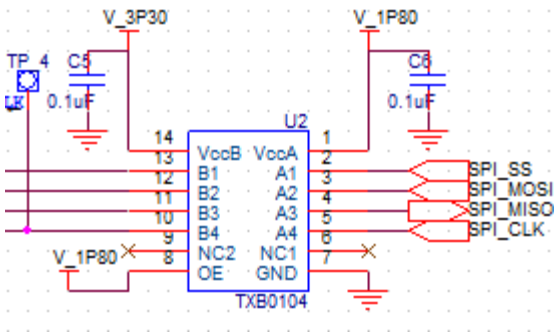

Figure 4. TXB0104 4-Bit bi-directional voltage-level translator.

The power supply for the AFE4490 was the most challenging design element. The AFE4490 needs a 5 V power supply for the LED driver, but the lithium polymer battery output (ranging from 3.7 V to 4.3 V) was insufficient. Therefore, a DC/DC boost converter was required to generate a 5 V power supply, as depicted in Figure 5.

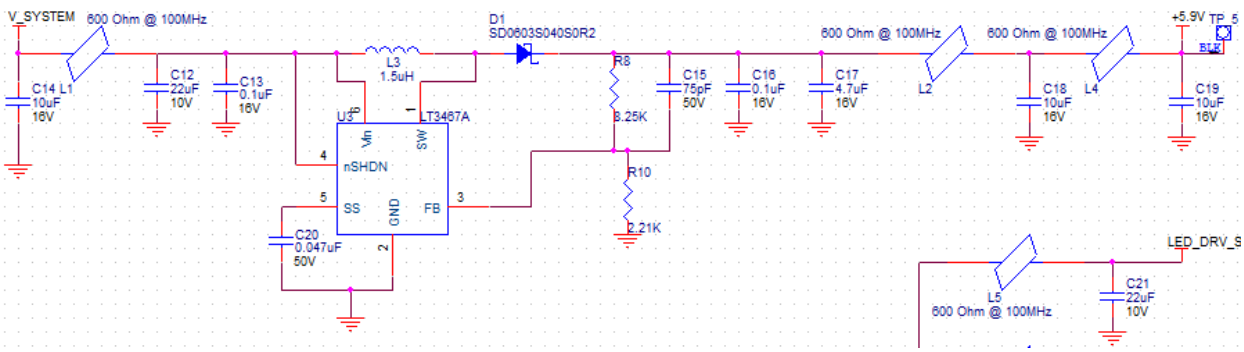

Figure 5. LT3467A DC/DC boost converter.

The Linear Technology LT3467A circuit illustrated in Figure 5 has an output of 5.9 V. A low-noise linear regulator is placed after the DC/DC boost converter to reduce noise. The Linear Technology LT3029 [13], depicted in Figure 6, is a dual low-noise linear regulator with outputs of 5 V and 3.3 V. The 5 V output powers the LED driving circuit in the AFE4490, and the 3.3 V output is used by the digital control circuit in the AFE4490 – see Figure 3.

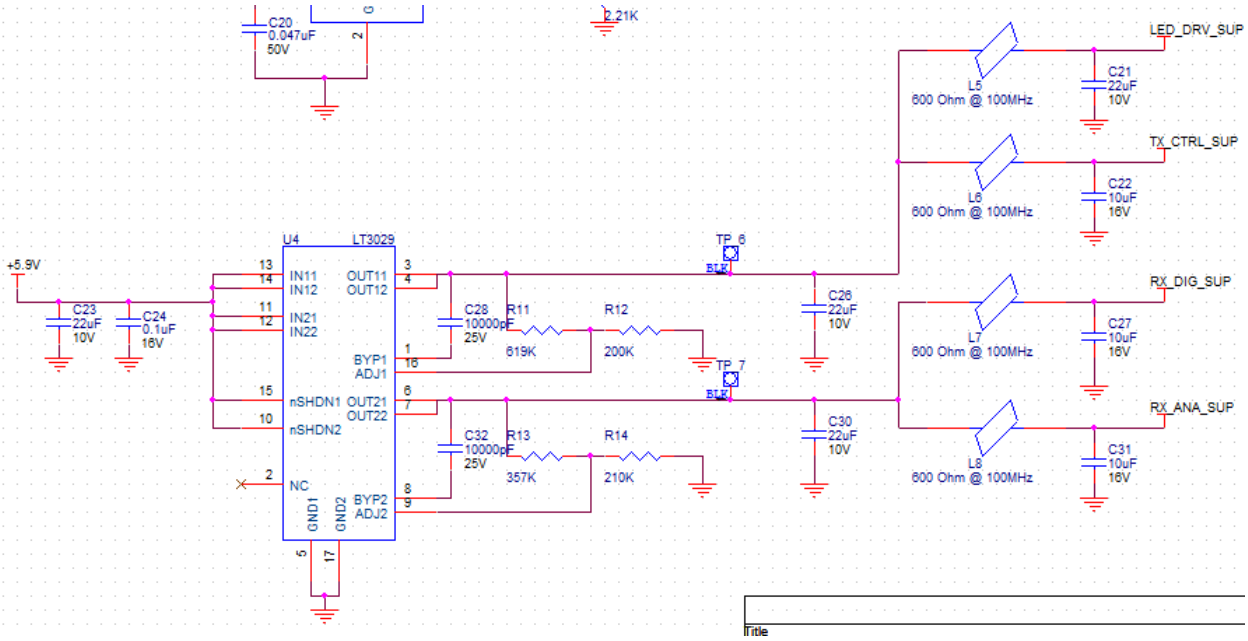

Figure 6. LT3029 dual low-noise linear regulator.

3.3 Accelerometer and Gyroscope

Accelerometer and gyroscope (gyrometer) sensors can be employed to track or predict activity intensity and potential fatigue. These sensors can be placed in locations such as the chest, leg, or wrist. Accelerometers and gyroscopes can also be used for motion detection or indication of artifacts, allowing a system to flag or ignore invalid ECG or PPG data.

The accelerometer and gyroscope sensor board (see Figure 7) was designed with an STMicroelectronics LSM9DS0 IC [14], which integrates a 3D accelerometer, a 3D gyroscope, and a 3D magnetometer. The interface between the Intel Edison and the LSM9DS0 is an I^2C link. The LSM9DS0 supports 1.8 V logic and requires a 3.3 V power supply.

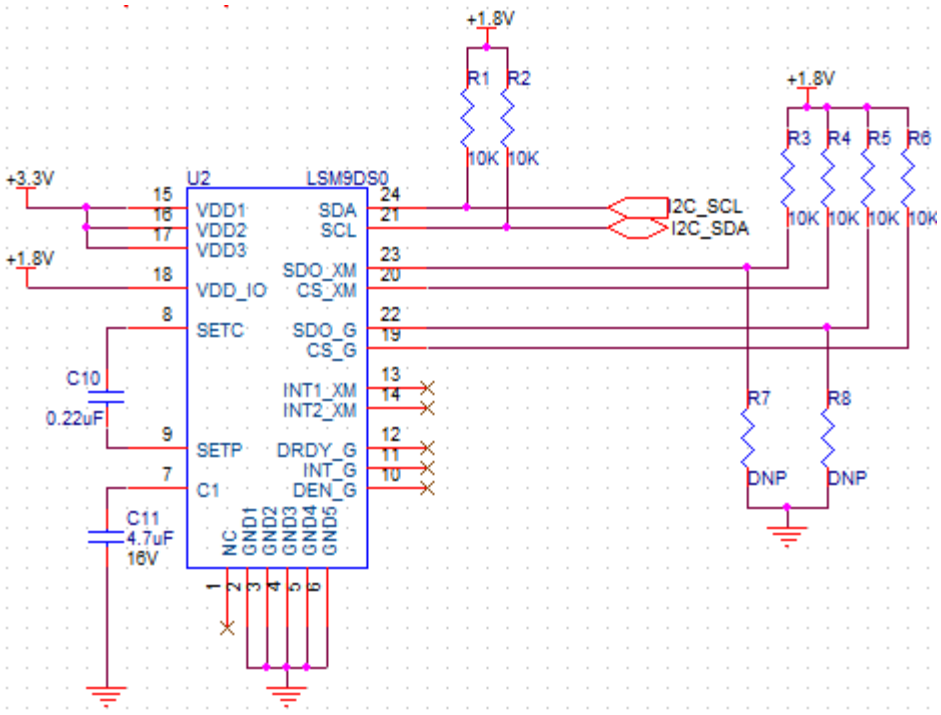

Figure 7. LSM9DS0 accelerometer and gyroscope sensor.

An Analog Devices ADP151AUJZ linear power regulator generated 3.3V of output power from a lithium polymer battery, and the Intel Edison sourced the 1.8 V of digital IO power, as illustrated in Figure 8.

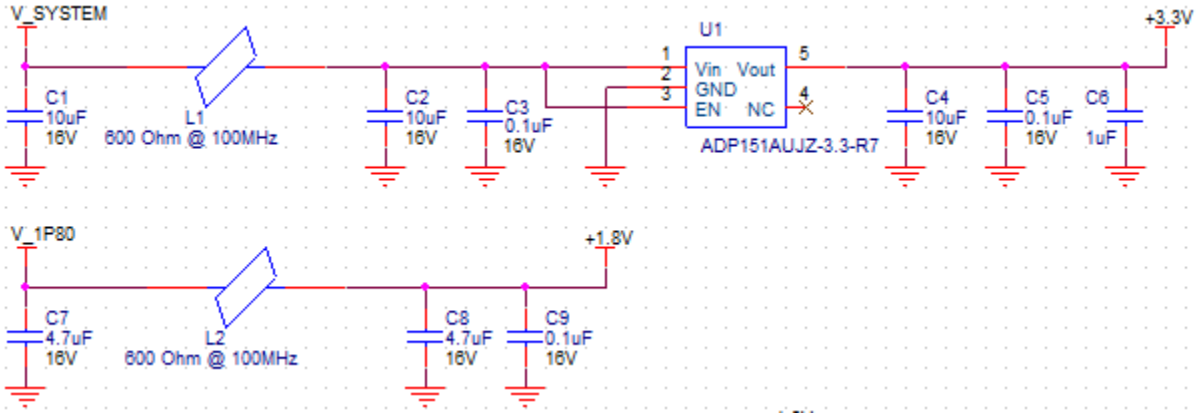

Figure 8. ADP151AUJZ power supply.

3.4 Interfaces and System Support Printed Circuit Boards

3.4.1 Battery and Serial Port Board

A battery and serial port board is required for any sensor setup in this stacked reference design. This board provides power and basic user interfaces, where LEDs and switches indicate and control wireless transfer and local storage modes. In a wired transfer mode, the battery and serial port board provides the serial port, power, and basic user interfaces (LEDs and switches). The battery and serial port board in this design is located opposite the Edison module: the sensor stack is sandwiched between the Edison unit and the battery and serial port board. The latter contains two switches and three LEDs for the basic user interface, plus two additional LEDs for the serial port. The implementation and usage of the battery and serial port board began with the change to version 3.0. The board contains a Microchip MCP73831 Li-polymer charge management controller [15] (Figure 9) and a Future Technology Devices International FT230X USB to basic UART IC [16] (Figure 10).

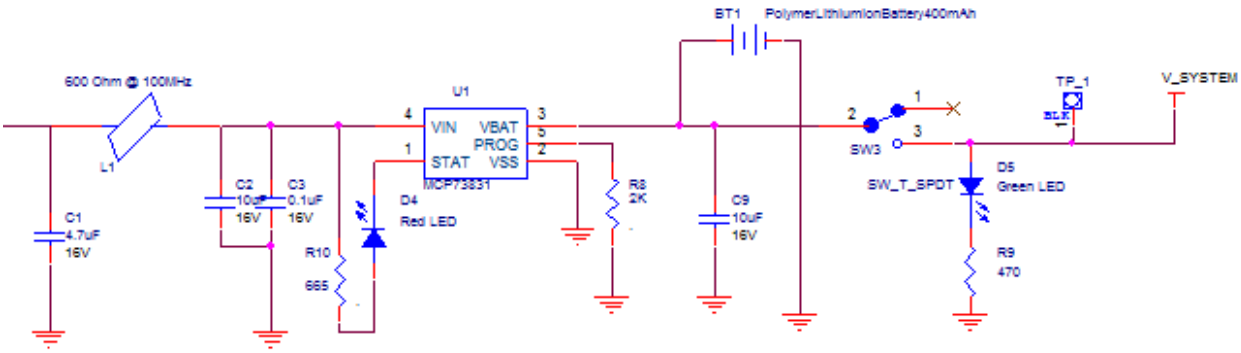

Figure 9. MCP73831 li-polymer charge management controller.

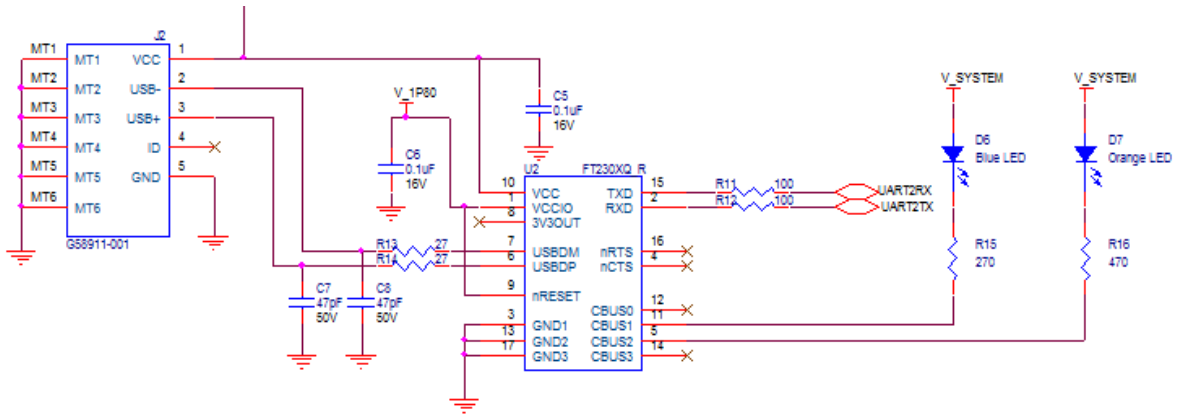

Figure 10. FT230X USB to basic UART IC.

In Figure 9, an R8 2 kΩ resistor was used to set the charge current at 500 mA. A green LED (D5) indicates power "ON," while a red LED (D4) indicates charging. SW3 is a system power switch. The FT230X (Figure 10) was configured to 1.8 V logic to match the digital input and output logic level on the Intel Edison. D6 and D7 LEDs indicate data transfer through the USB port. Three LEDs were configured to display working conditions, such as wireless or wired mode, and active sensors. Two switches (SW1 and SW2) select different working modes or set different sampling frequencies. Figure 11 illustrates these switches and LED indicators in more detail.

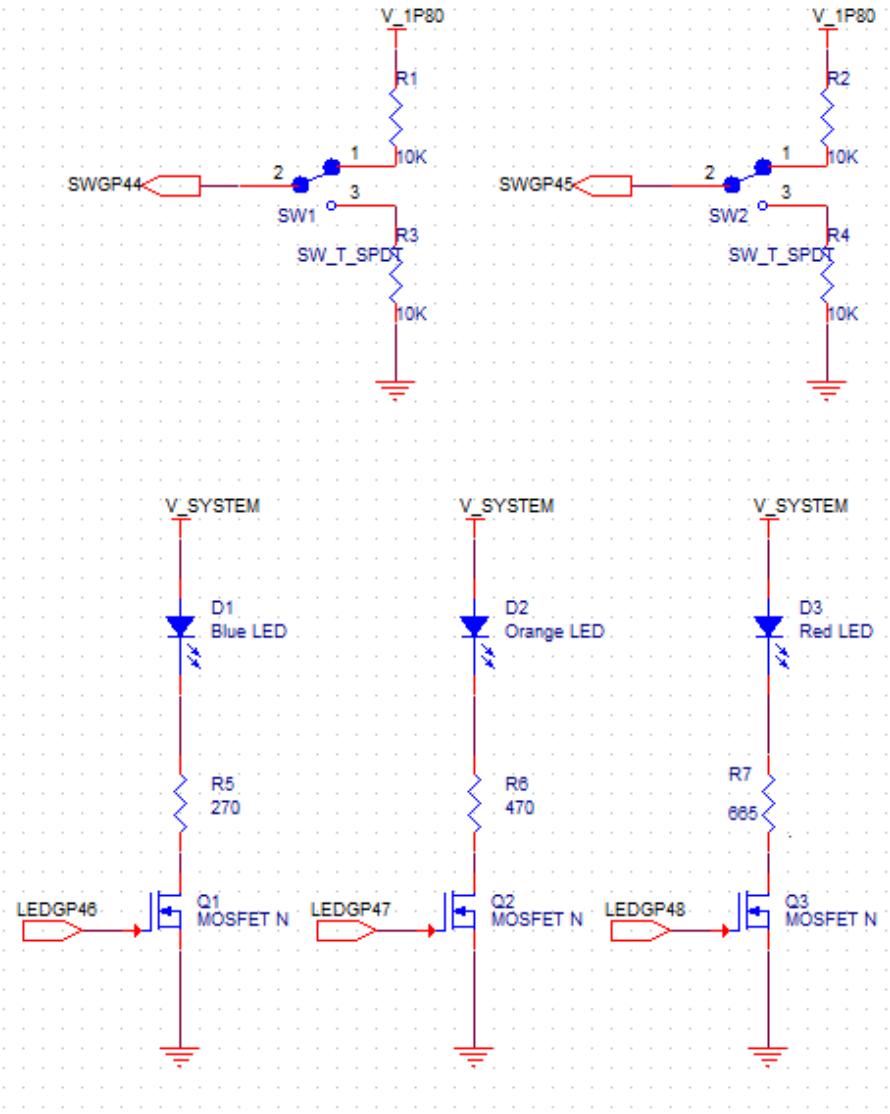

Figure 11. Switches and LED indicators.

3.4.2 Reflection-Mode Pulse Oximetry Sensors

Reflection-mode pulse oximetry sensors can be used in various locations on the human body. Two designs for reflection-mode pulse oximetry sensors have been common in prior KSU work. In 2010, Kejia Li utilized the first design, where four photodiodes surround a central pair of red and IR emitter LEDs. This layout maximizes the capture of the reflected photons. The

corresponding schematic and PCB layout for the present effort are depicted in Figures 11 and 13, respectively.

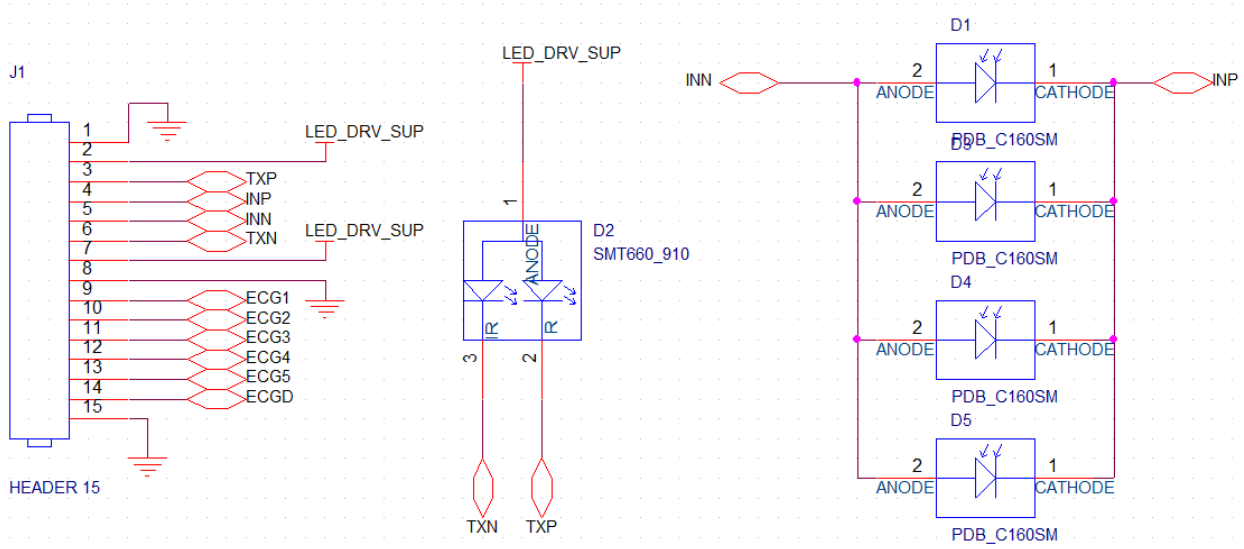

Figure 12. Schematic for a reflection-mode pulse oximetry sensor (quad photodiodes).

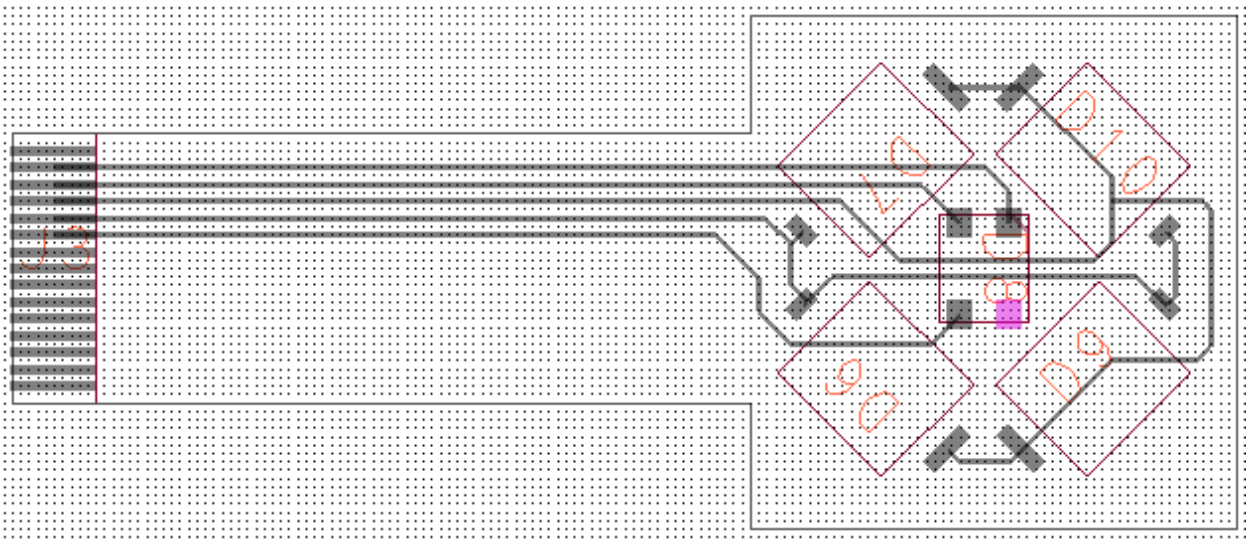

Figure 13. PCB layout for a reflection-mode pulse oximetry sensor (quad photodiodes).

The second design utilizes a single photodiode in the same package with the emitter LEDs – see Figures 14 and 15 for the corresponding schematic and PCB layout, respectively. Because this design has a layout that is similar to most commercial reflectance pulse oximetry sensors, the resulting signals can sensibly be compared to signals obtained using the quad photodiode design. In this research, the single photodiode sensor also serves another purpose as a ECG sensor debugging tool. Because the lower set of connection pads are not needed for the single photodiode sensor (refer to the left side of Figure 15), these pads are connected to four test points (gray circles in Figure 15). This allows the flexible PCB to instead be plugged into an ECG board within the sensor stack and then be used for ECG testing purposes.

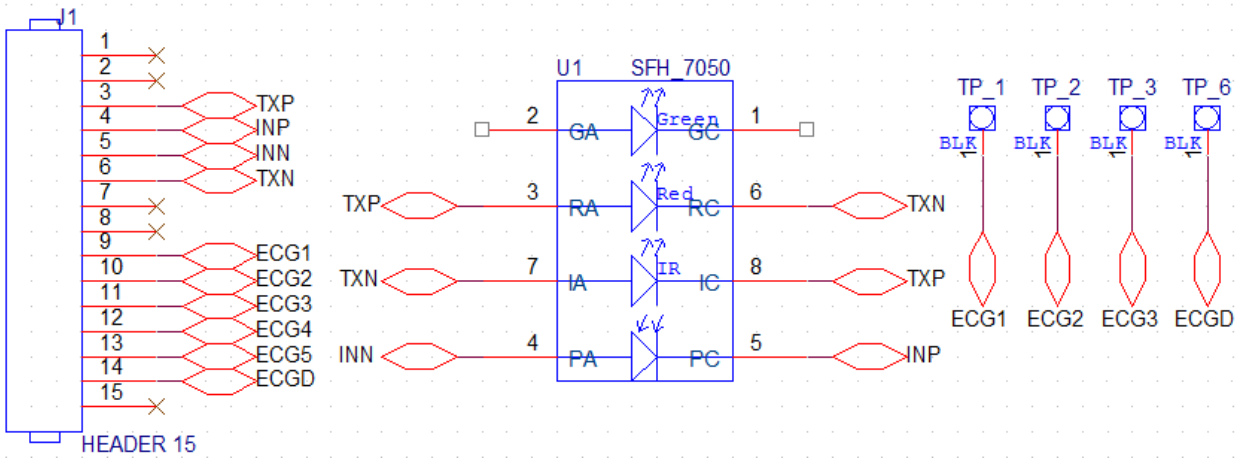

Figure 14. Schematic for a reflection-mode pulse oximetry sensor (single photodiode).

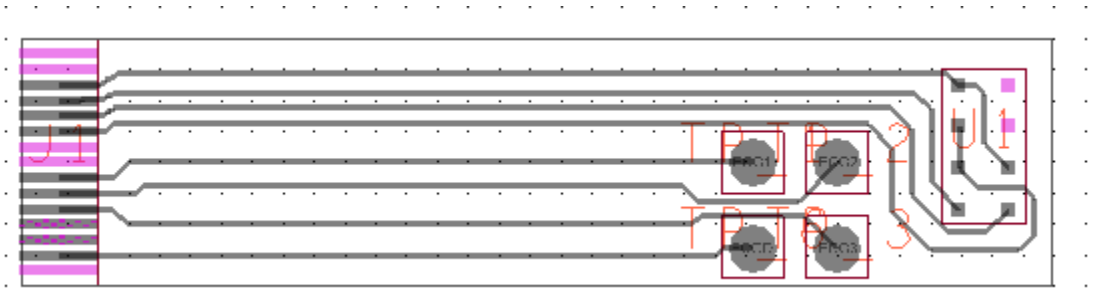

Figure 15. PCB layout for a reflection-mode pulse oximetry sensor (single photodiode).

3.4.3 Commercial Pulse Oximetry Sensor Adaptor

A sensor adapter was used to enable commercial pulse oximetry sensors to be plugged into the pulse oximeter board. The Nellcor DP9 sensor [17] was selected based on the ease to interface with the sensor, its cost, and the supply stability.

3.4.4 Commercial ECG Lead Adaptor

A commercial ECG lead adaptor was used to enable commercial ECG leads to be plugged into the ECG board. The Philips 15 pin sensor [18] was selected based on the ease to interface with the sensor, its cost, and the supply stability.

Chapter 4 - Hardware and Manufacturing

Due to the stackable and extendable design, all printed circuit boards need to be the same size as the Intel Edison unit. The physical dimensions of the Intel Edison are 35.5 mm × 25.0 mm × 3.9 mm, as depicted in Figure 16 [7].

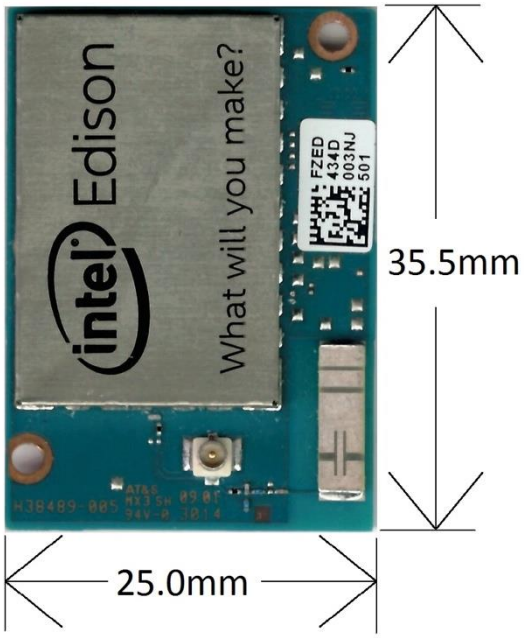

Figure 16. Intel Edison physical dimensions.

For each sensor board, the positions of the 70-pin connector, mounting holes, and antenna keep-out zone are designed to align with the corresponding positions on the Intel Edison. Figures 17 through 21 contain pictures of the device hardware.

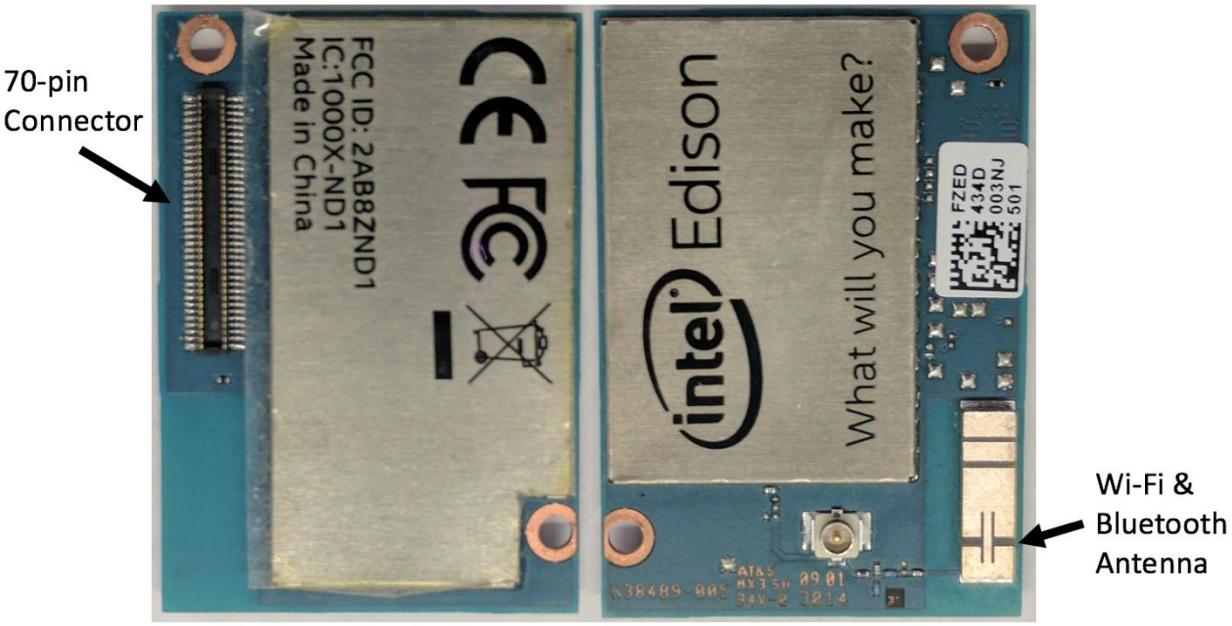

Figure 17. Intel Edison package front and back.

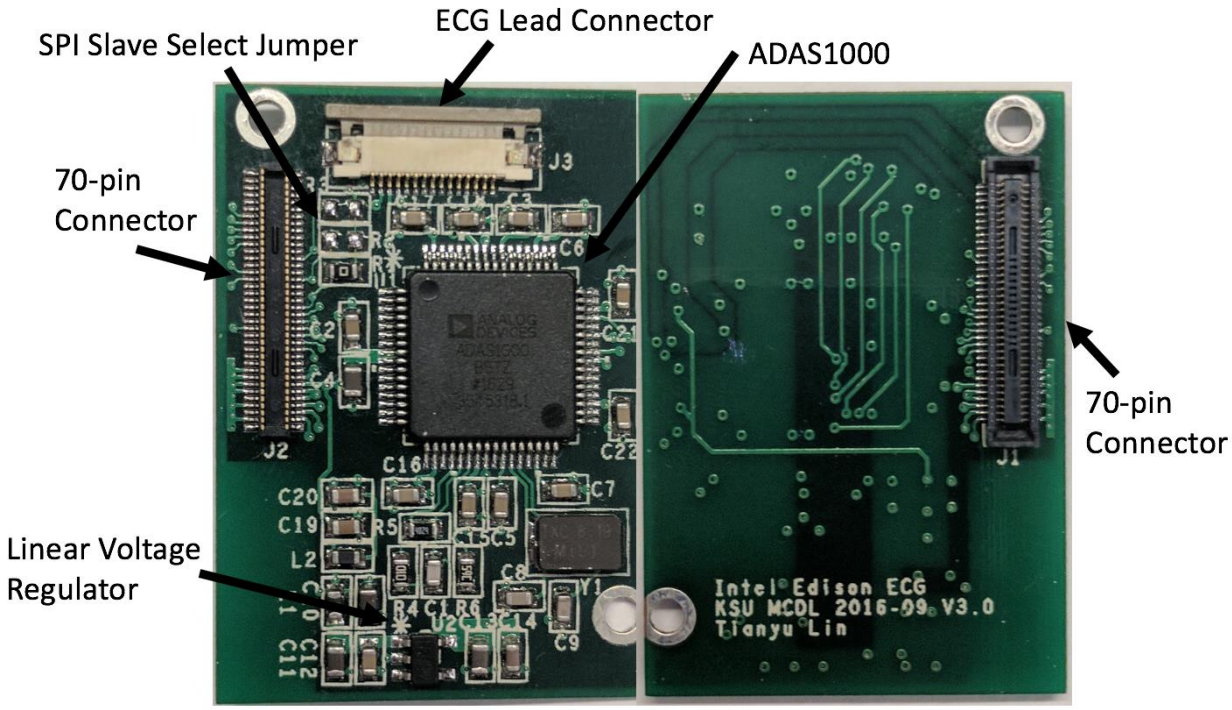

Figure 18. ECG sensor PCB front and back.

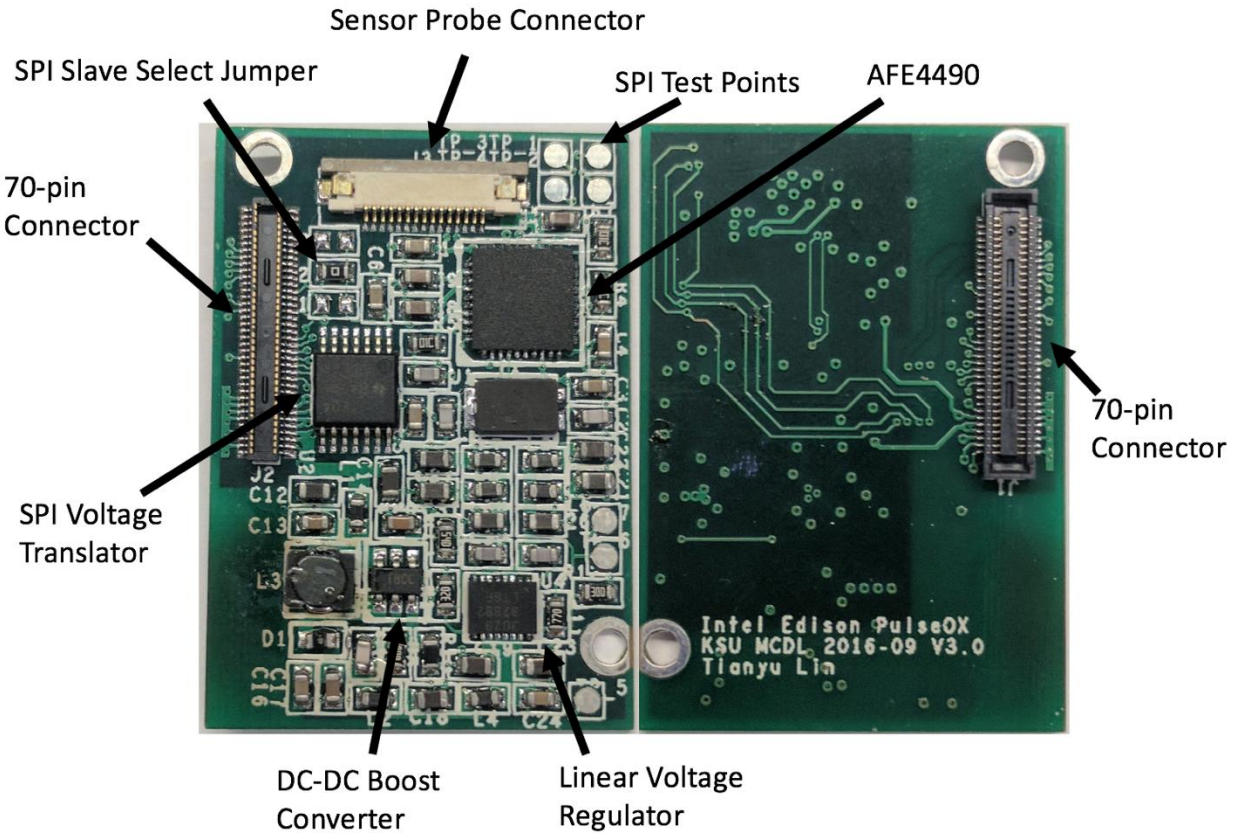

Figure 19. Pulse oximeter sensor PCB front and back.

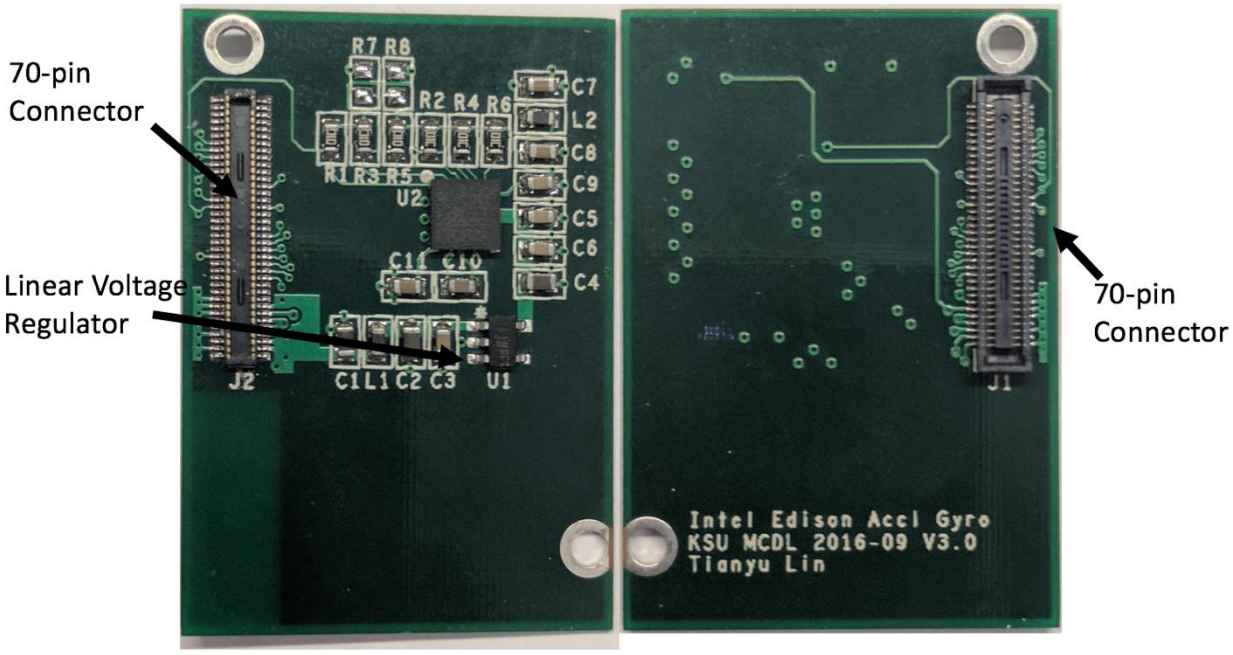

Figure 20. Accelerometer and gyroscope sensor PCB front and back.

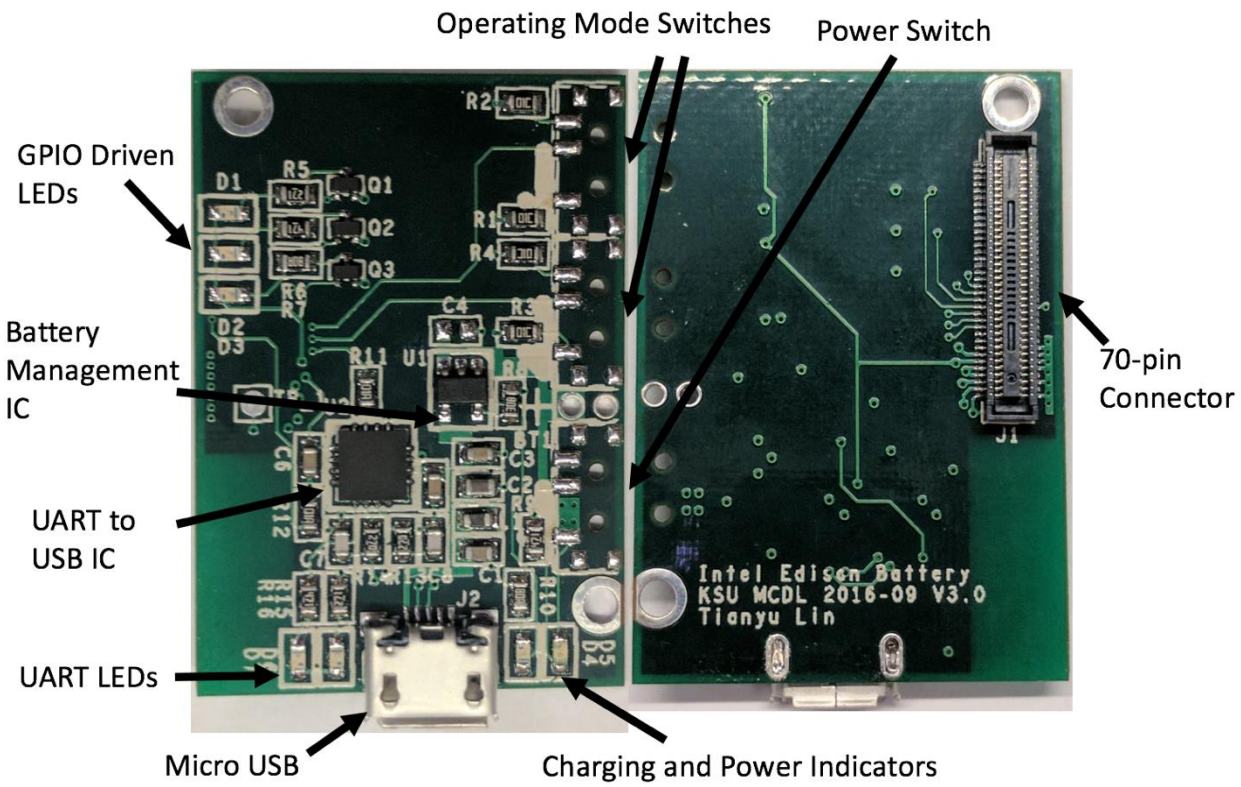

Figure 21. Battery and serial port PCB front and back.

Figure 22 contains a picture of the two reflectance sensor probes created for the pulse oximeter board. In Figure 22, the single photodiode design minimizes the space between the LEDs and the photodiode, resulting in potential ultra-low-power consumption. The quad photodiode design maximizes received light energy, potentially increasing sensitivity.

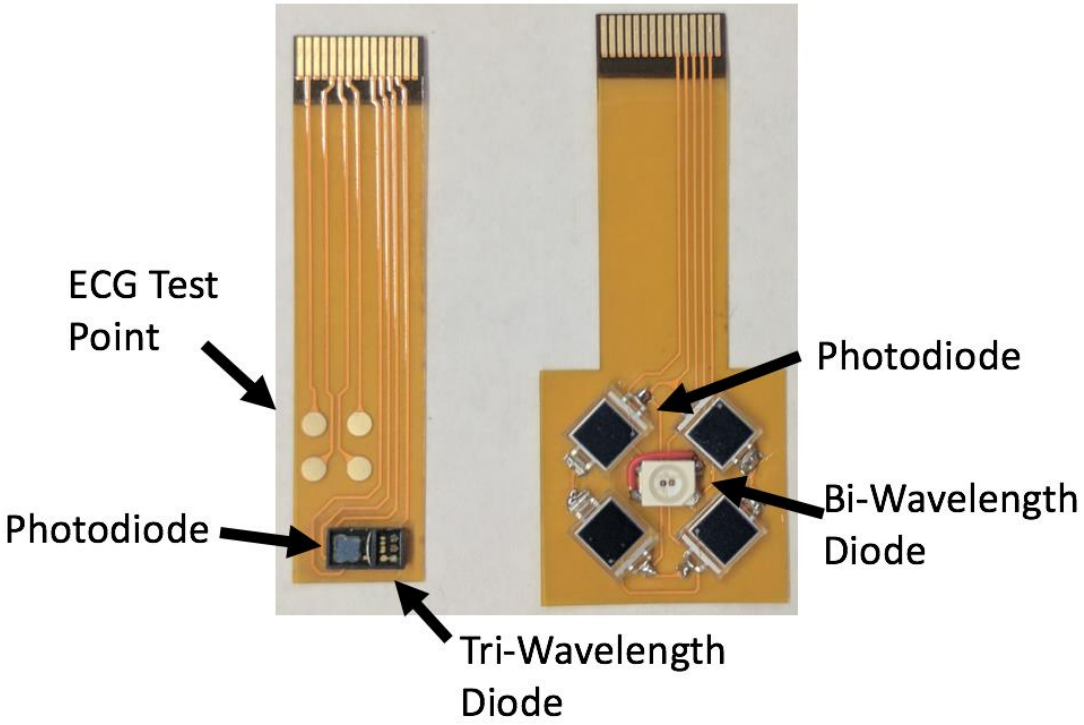

Figure 22. Single photodiode and quad photodiode sensor probes.

Figure 23 depicts a side view of the device and sensor stack, where only one sensor is employed. From the top to the bottom, as shown in the figure, the layers are a lithium polymer battery, a battery and serial port PCB, a sensor PCB with a sensor probe, and an Intel Edison unit, respectively.

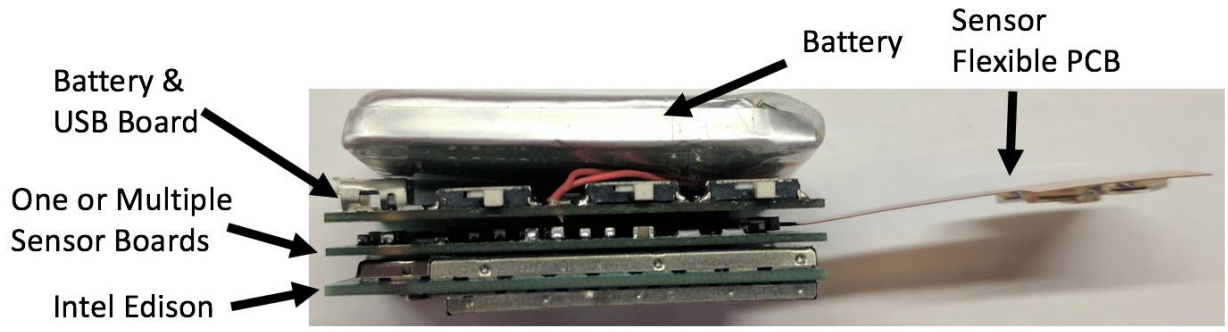

Figure 23. Side view of a one-sensor stack.

Chapter 5 - Firmware Development

5.1 Software Flow

To achieve plug and play usability, the firmware must be able to detect the sensor type and the number of attached sensors. The software flow diagram is illustrated in Figure 24.

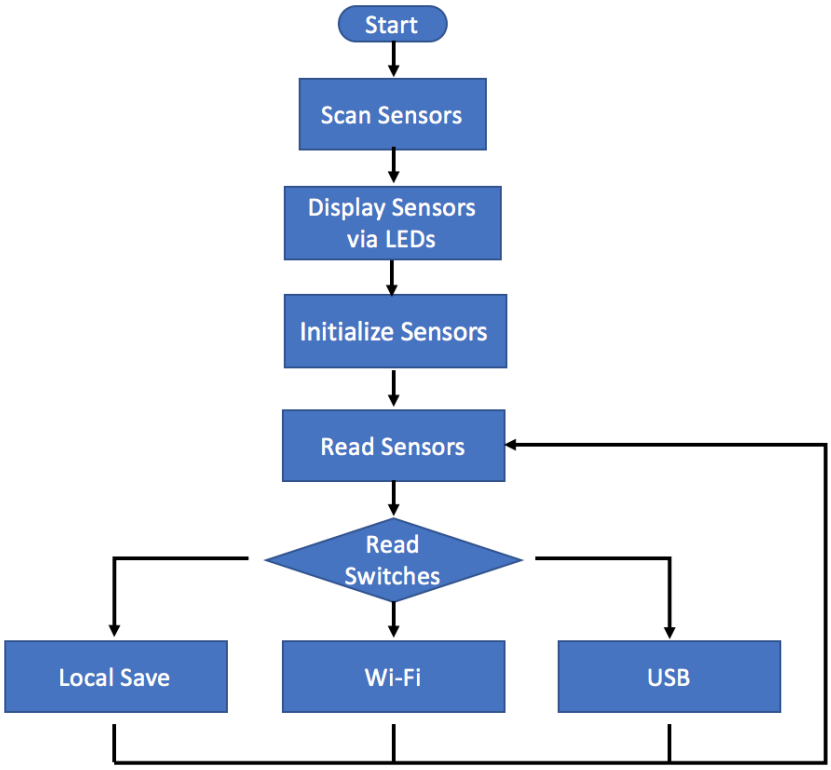

Figure 24. Software flow diagram.

Immediately after initiating the software, the program automatically cycles through all possible slave selects on the ISP interface and then cycles through all possible addresses on the I^2C interface. The present sensors are displayed via the LEDs on the battery and serial port PCB, and the Intel Edison automatically initializes all attached sensors. The Intel Edison then reads out sensor values and inputs from the slide switches on the battery and serial port board in order to select data transfer modes.

Three transfer modes are available: local storage, Wi-Fi streaming, and USB streaming. Local storage can be accessed through Wi-Fi via FTP software. All data points are stamped with the system time to avoid an unnoticed missing data point. The software continues to acquire data until the system powers down or the stop command is utilized. The local save mode saves the time-stamped data in a text file format on the Intel Edison's internal flash memory. Local storage offers the advantages of reliability and a high sampling rate. Once data collection is complete and the Intel Edison is connected to a Wi-Fi hotspot, the saved file can be accessed through FTP client software on a personal computer or smartphone.

Wi-Fi streaming uses a secure shell (SSH) to access the serial port for data streaming. USB streaming is similar to Wi-Fi streaming in that a USB COM port is provided by an FT230X USB to basic UART IC (Figure 10). Both modes allow access to the Linux command line.

5.2 Simplified Preconfigured Program

The system typically has one or two known sensors, so the data transfer mode will also be preconfigured in the code. This simplified program can optimize power consumption and sampling rate. As an example, a 'local save' preconfigured flowchart is depicted in Figure 26. As soon as the program begins, the system ensures that sensors are present and initialized. Then, it loops through reading and save modes until the system powers down or the stop command is utilized.

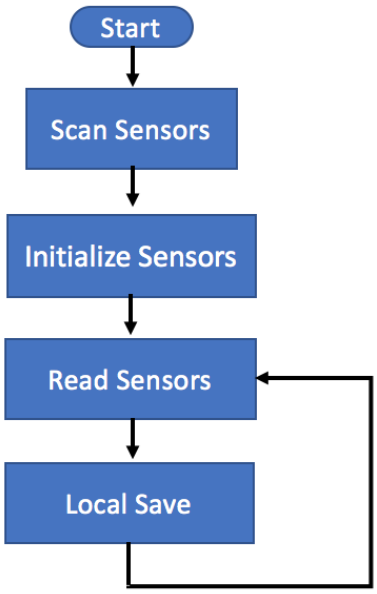

Figure 25. Simplified preconfigured program flowchart.

Chapter 6 - Results and Analysis

6.1 Electrocardiograph

The ECG data in Figure 26 were acquired in a three-lead configuration. The *x*-axis represents time in seconds, and the *y*-axis shows digital levels. In the legend in the upper right corner, *LA* means left arm, *LL* means left leg, and *RA* means right arm. An independent reference ground was not employed.

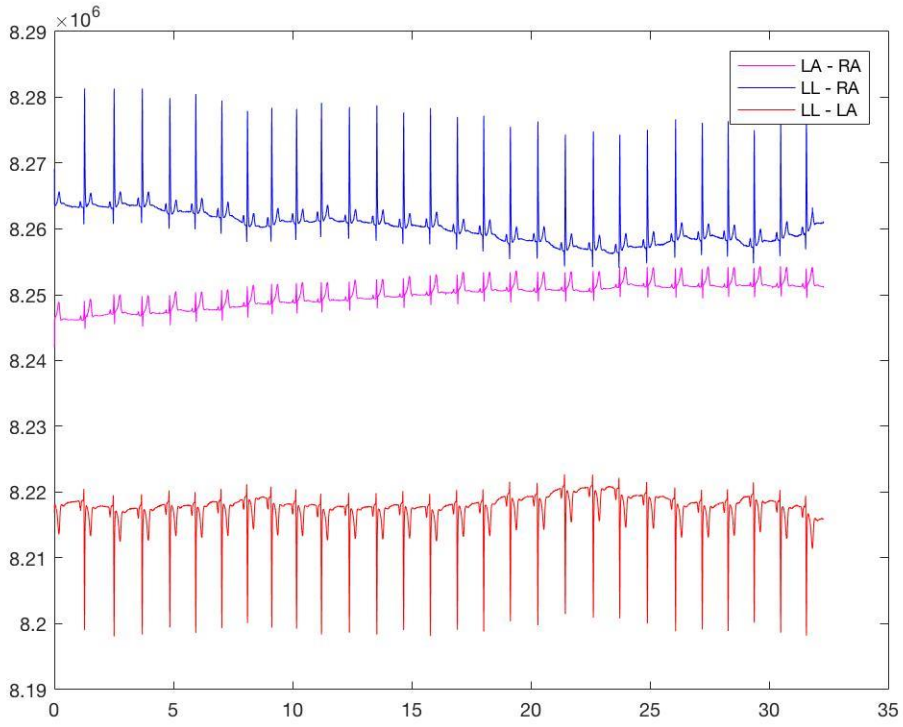

Figure 26. Three-lead ECG sample data.

These data were acquired over 32.29 seconds, which included 28 cardiac pulse intervals, corresponding to a heart rate of 52 beats per minute. The *x*-axis represents 25,642 data points for each channel, over a time interval of 32.29 seconds, meaning a sampling rate of 794 Hz. A

standard clinical ECG system assumes spectral information between 0.05 Hz and 100 Hz [19], so this sampling rate is adequate to capture several harmonics of the highest frequency components.

Figure 27 presents zoomed-in plots for each of the three leads (channels), where the LL-RA channel and the LL-RA channel exhibit 20,000 digital levels peak to peak, and the LA-RA channel demonstrates 5,000 digital levels peak to peak. These levels represent suitable precision for the wearable applications where these wireless systems will be utilized.

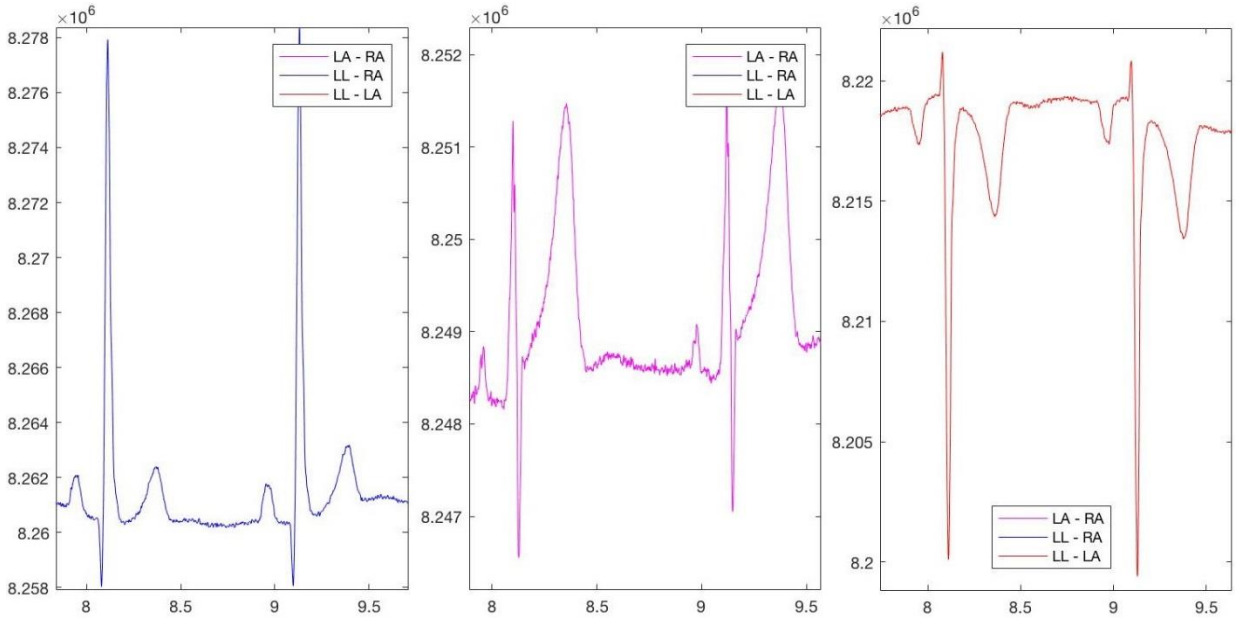

Figure 27. Three-channel ECG zoomed-in plots.

Figure 28 presents a single-sided amplitude spectrum for the LL-LA channel. Spectra for the LL-RA channel and the LA-RA channel are similar. For this data set, the lowpass filter in the ADAS 1000 was set to 250 Hz. No visible 60 Hz noise was evident in the spectrum, eliminating the need for an additional digital low-pass filter. Figure 29 presents a zoomed-in plot for observation of the fundamental frequency: 0.88 Hz, or 53 pulses per minute, which matches the previous calculation.

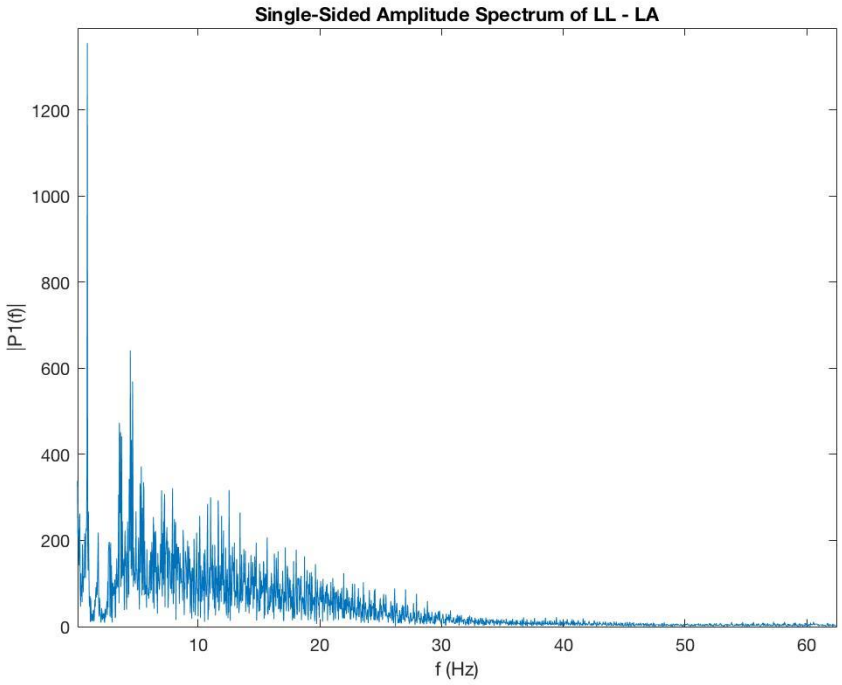

Figure 28. Single-sided amplitude spectrum for the LL-LA channel.

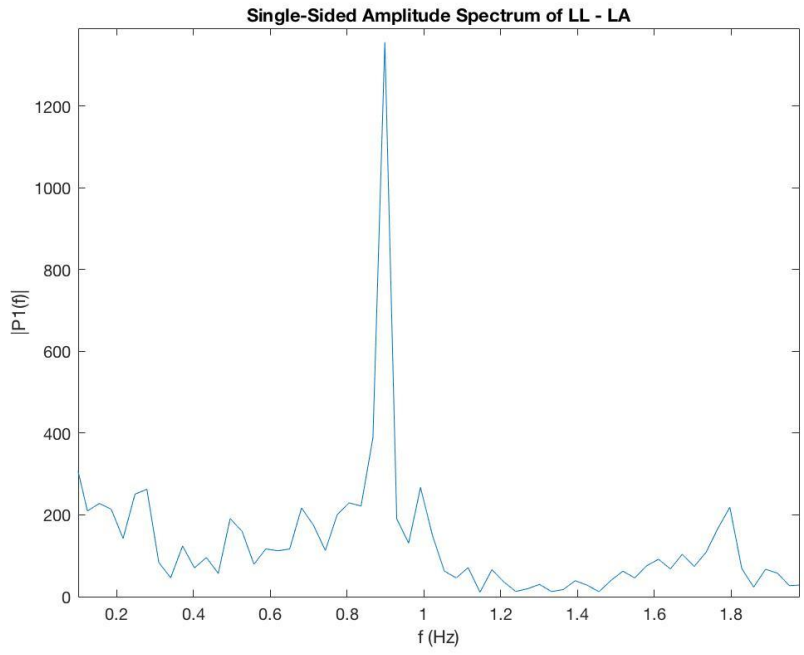

Figure 29. Zoomed-in, single-sided amplitude spectrum for the LL-LA channel.

6.2 Pulse Oximeter

Three types of pulse oximeter sensor probes were tested and/or developed: a transmissivity-type commercial finger-clip probe, a reflective quad-photodiode flexible PCB probe, and a reflective single-photodiode flexible PCB probe. The signals depicted in Figure 30 are the photo-plethysmograms (PPGs) obtained from the red and infrared channels of a commercial Nellcor finger probe. Each signal is clean, with the exception of one outlying point at 7.7 sec on the IR channel. A total of 33 pulses are recorded in 30 seconds, yielding a heart rate of 66 beats per-minute.

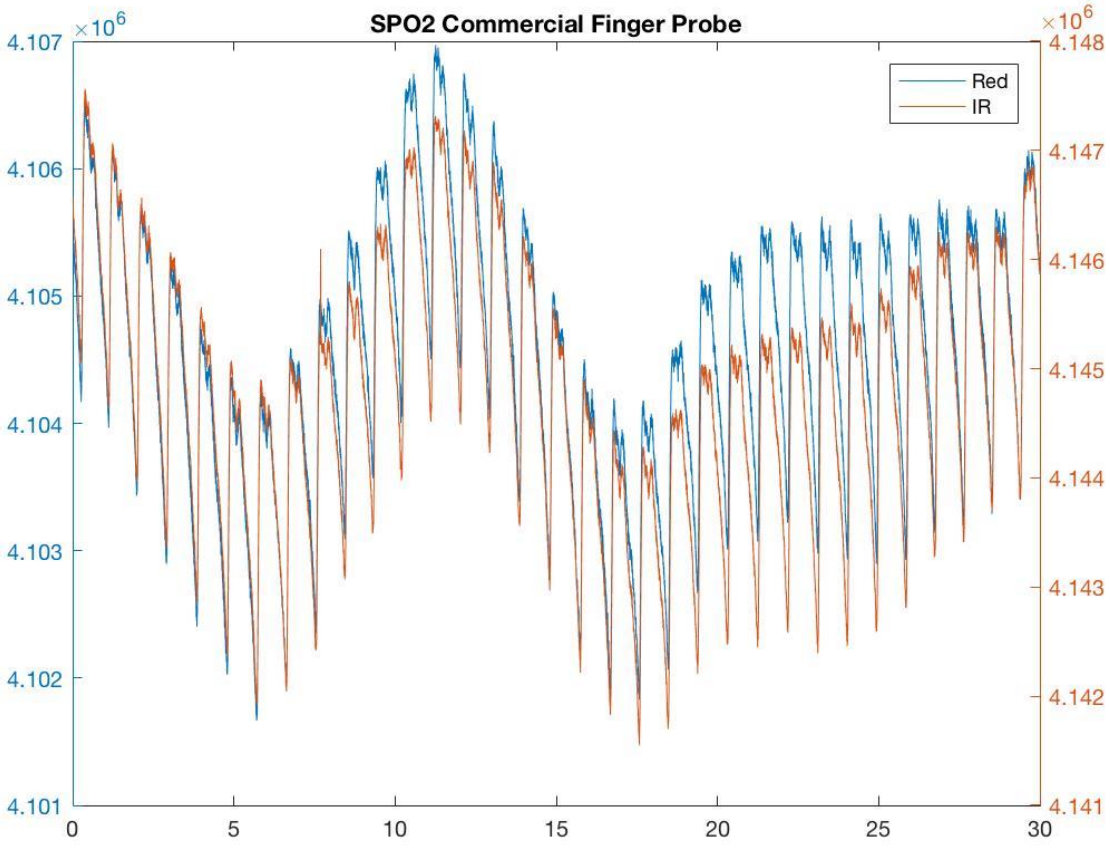

Figure 30. PPGS obtained with a commercial finger probe.

PPG spectra from the red and infrared channels are similar to one another. Figure 31 presents the amplitude spectrum for the red PPG. For this data set, the lowpass filter in the AEF4490 was set to 500 Hz. Very little 60 Hz noise is observed in the spectrum, eliminating the need for an additional digital low-pass filter.

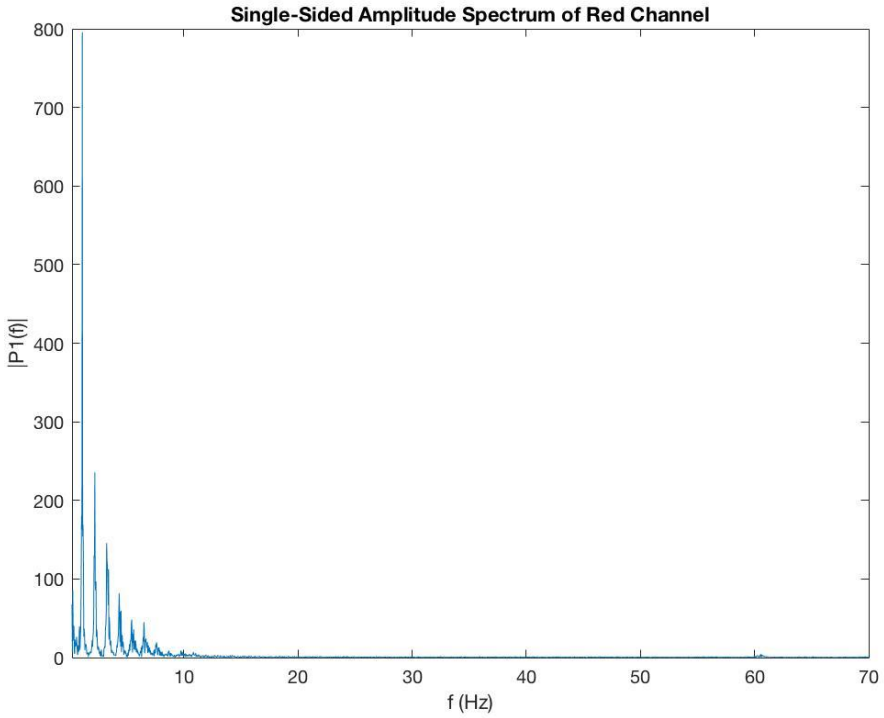

Figure 31. FFT-based amplitude spectrum for a red PPG obtained with the commercial finger probe.

Figure 32 presents a zoomed-in plot for close observation of the fundamental frequency: 1.1 Hz, or 66 beats per minute, which matches the previous calculation.

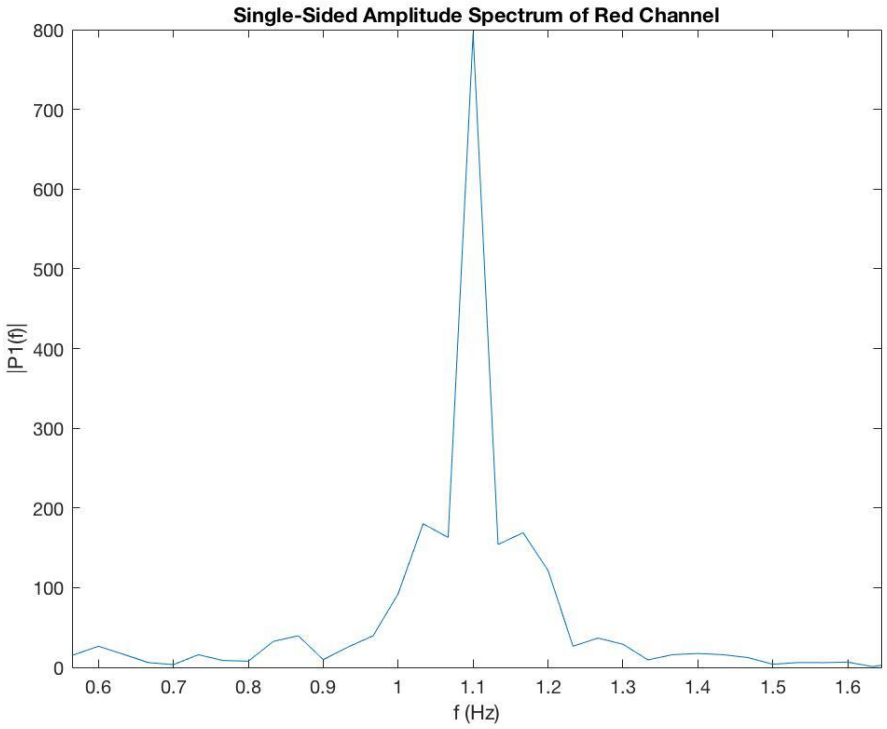

Figure 32. Zoomed-in amplitude spectrum for the infrared PPG (commercial finger probe).

There was a compromise between the gain settings required for the transmissivity-type commercial finger probe, the reflective quad-photodiode probe, and the reflective single-photodiode probe. All data were acquired with the same gain setting. Approximately 2,000 peak-to-peak digital levels were evident in the red PPG data acquired with the transmissivity-type commercial finger probe, whereas 2500 digital levels were evident for the infrared PPG. Approximately14,000 peak-to-peak digital levels were evident in the red PPG data acquired with the reflective quad-photodiode probe, whereas 25,000 digital levels were evident for the infrared PPG. Approximately 800 peak-to-peak digital levels were evident in the red PPG data acquired with the reflective single-photodiode probe , whereas 1,200 digital levels were evident for the infrared PPG.

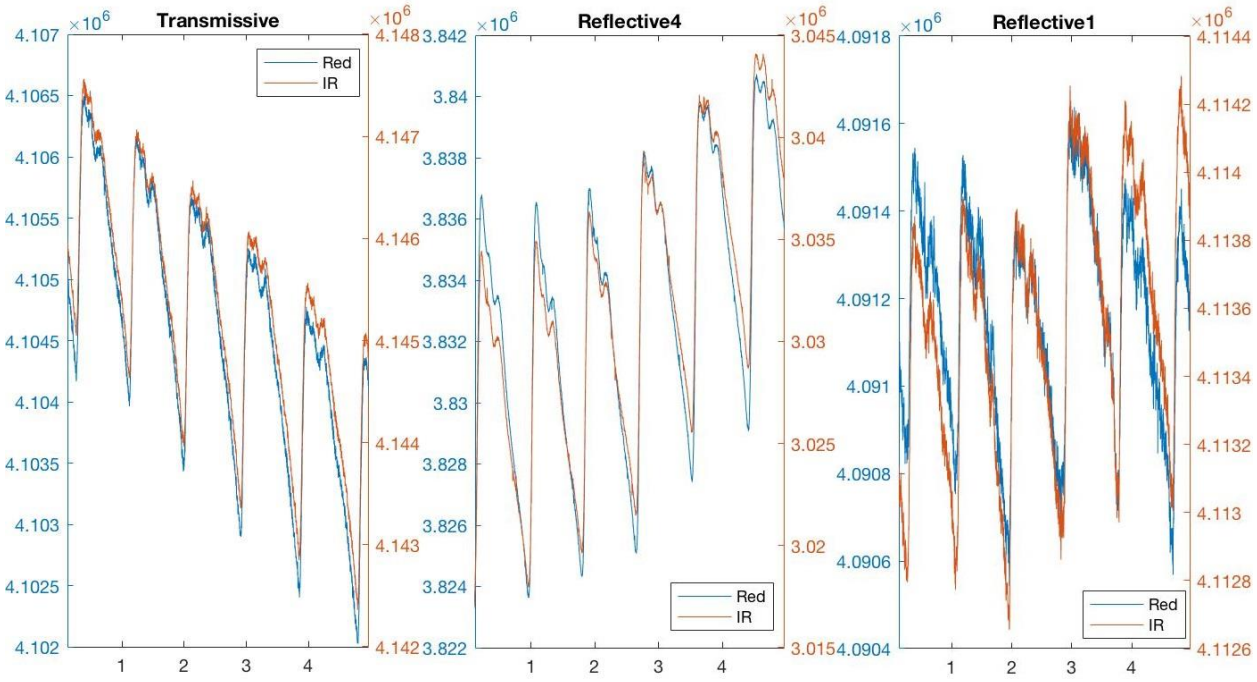

Figure 33. PPG plots for the transmissive commercial finger probe, the reflective quad-photodiode probe, and the single-photodiode probes.

Based on the spectra of the PPGs acquired with the three different sensor probes, the reflective quad-photodiode probe demonstrated significantly higher sensitivity than the other probes – see Figure 34. All PPGs demonstrated little energy above 10 Hz.

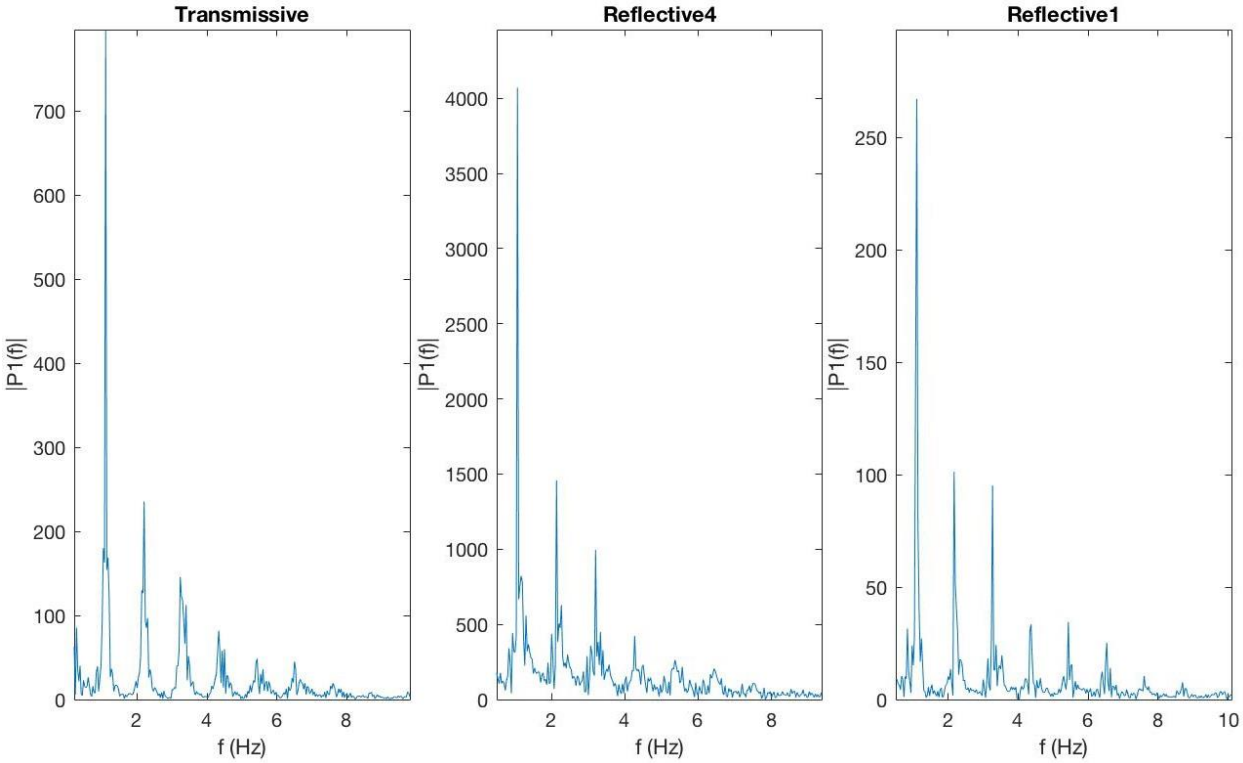

Figure 34. Amplitude spectra for the transmissive commercial finger probe, the reflective quad-photodiode probe, and the single-photodiode probes.

6.3 Accelerometer and Gyroscope

For an initial test, the accelerometer and gyroscope were rotated twice in the same direction; each rotation was 90 degrees. The resulting accelerometer plot in Figure 35 starts with -1 g on the *z*-axis, and then 1 g is evident on the *y*-axis after one 90-degree rotation. Finally, 1 g is evident on the *z*-axis after an additional 90-degree rotation. These results indicate that the accelerometer and gyroscope pair is working properly.

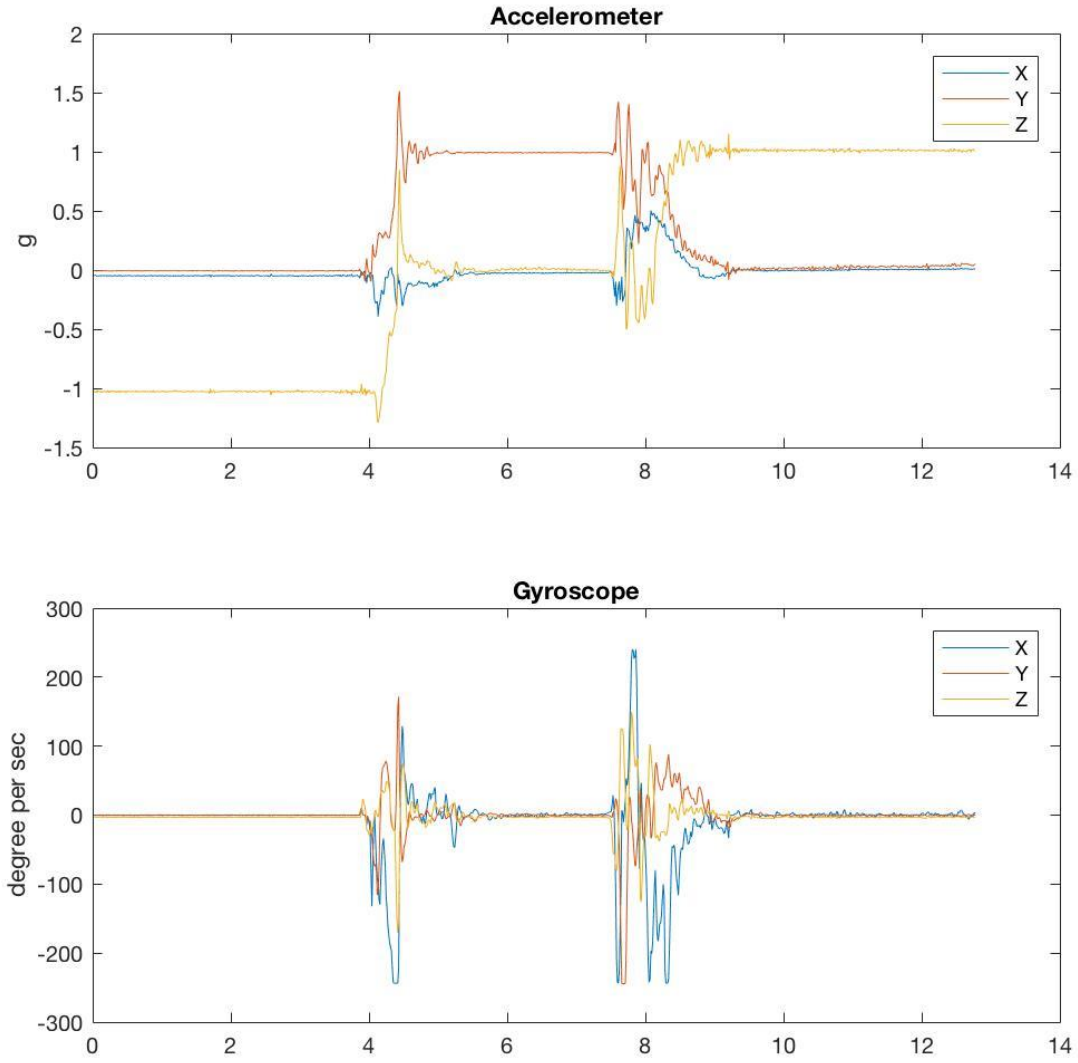

Figure 35. Accelerometer and gyroscope signals.

6.4 Power Consumption

Power consumption is a crucial parameter for a battery powered device, as operation times affect wearability, practicality, and user acceptance in different usage environments. The power consumption testing method involves picking three different power supply voltages within the range of a lithium polymer battery: 4.3 V, 4.0 V, and 3.7 V. Current draw is measured with a benchtop multimeter at each excitation voltage, and then the resulting three powers are averaged. The power consumption test results are listed in Table 2.

Table 2. Power consumption.

Component Configuration	Power Consumption (mW)
Intel Edison Idle	279
Active Wi-Fi	205
Active ECG sensor	271
Active SpO2 sensor	554
Active Accelerometer, Gyroscope	78

The battery on the battery and serial port board had a power rating of 1480 mWh. As an example, the run time for the ECG sensor operating in local saving mode can be calculated as 1480 / (279+271) = 2.69 hours.

6.5 Sampling Rate Variation

The sampling rate can vary for different reasons. The version of Linux that runs on the Intel Edison is a non-real-time operating system, which makes it necessary to assess variations in the sampling rate in order to gain confidence in the robustness of the resulting signals. For an initial assessment, ECG data were acquired and time stamped for forty minutes. The resulting histogram of sampling intervals is presented in Figure 36. The average sampling interval is 3.5 ms with a standard deviation of 0.342 ms.

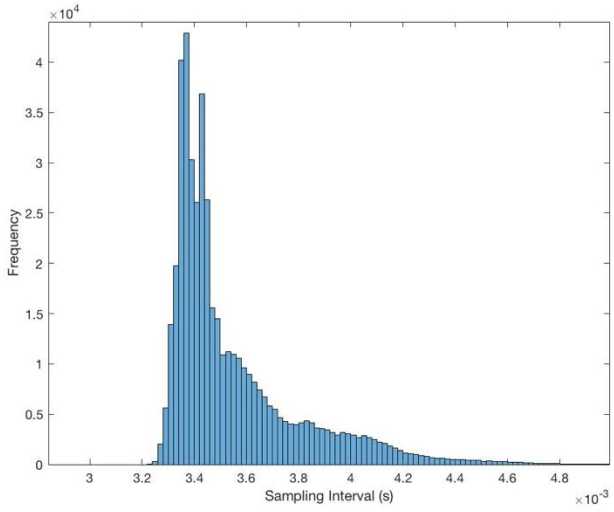

Figure 36. Histogram of sampling intervals.

Chapter 7 - Conclusion

This Intel Edison-based design demonstrated the feasibility of a battery powered, wireless, modular biomedical device whose stack of one or more sensors can be easily reconfigured depending upon the needs of the monitoring application. If the application needs multiple types of biomedical data at the same time, these data will be synchronous by nature – a hard requirement to meet when different devices controlled by different computers are worn at the same time. This Edison-based design can be used as a reference design for new sensor development related to data acquisition devices intended for biomedical signal analyses and educational purposes.

With the exception of the respiration belt sensor, which was removed from the design early on, all of the planned sensors were tested and function as designed. In the case of the pulse oximeter, the flexible PCB sensor adapter provides the convenience to use various kinds of mass production sensor probes without cutting wires and soldering.

The software running on the Intel Edison is based on the Python programing language. The command terminal and file system used by the Intel Edison unit can be operated remotely, making software updates possible to implement during wireless data acquisition. The data visualization and analysis programs utilized for this work were developed in MATLAB.

The development process offered challenges related to miniaturization and modularity. In terms of miniaturization, the dimensions of the Intel Edison constrained the dimensions of the sensor PCBs. To minimize thickness, the surface-mount components were only placed on one side of each sensor PCB. These limited physical dimensions posed a challenge for the ECG and pulse oximeter sensor designs. The modular design requires a high pin count and a fine-pitch connector, which make these parts difficult to solder.

These challenges resulted in four design revisions. Future development will involve the creation of additional sensors, including a humidity, temperature, and pressure sensor that can provide information about the operational environment of any other sensors in the stack. Creative casing designs will also be required that can accommodate changing in device thickness depending on the numbers of stacked sensors employed. Analyses will also be needed to assess the effects of sampling rate variations on signal integrity and usability.

Chapter 8 - References

[1] Jianchu Yao, Design of standards-based medical components and a plug-and-play home health monitoring system, Manhattan, Kansas: K-State Electrical & Computer Engineering, 2005.

[2] Kejia Li, "Wireless reflectance pulse oximeter design and photoplethysmographic signal processing," Manhattan, 2010.

[3] Kejia Li and Steven Warren, "GumPack: a personal health assistant with reconfigurable surface components," *Journal of Healthcare Engineering*, vol. 4, no. 1, pp. 145-166, 30 8 2012.

[4] Xiongjie Dong, "A ZigBee-based wireless biomedical sensor network as a precursor to an in-suit system for monitoring astronaut state of health," Manhattan, 2014.

[5] Arduino, "Arduino mkr1000," 5 1 2017. [Online]. Available: https://store.arduino.cc/usa/arduino-mkr1000. [Accessed 25 7 2017].

[6] Raspberry Pi Ltd., "Raspberry Pi," 13 10 2016. [Online]. Available: https://www.raspberrypi.org/documentation/hardware/computemodule. [Accessed 25 7 2017].

[7] Intel Corporation, "Intel® Edison Compute Module Hardware Guide," Jan. 2015. [Online]. Available: http://download.intel.com/support/edison/sb/edisonmodule_hg_331189004.pdf . [Accessed 10 January 2017].

[8] RFduino, "RFD22102 RFduino DIP," 12 5 2013. [Online]. Available: http://www.rfduino.com/product/rfd22102-rfduino-dip/index.html. [Accessed 25 7 2017].

[9] Devon Krenzel, Steve Warren, Kejia Li, Natarajan Bala and Gurdip Singh, "Wireless slips and falls prediction system," 12 12 2012. [Online]. Available: http://ieeexplore.ieee.org/document/6346854/. [Accessed 23 5 2017].

[10] Analog Devices, "Low Power, Five Electrode Electrocardiogram (ECG) Analog Front End" ADAS1000 datasheet, Aug. 2012 [Revised Jun. 2014] Available: http://www.analog.com/en/products/analog-to-digital-converters/adas1000.html.

[11] Analog Devices, "Ultralow Noise, 200 mA, CMOS Linear Regulator" ADP151 datasheet, Mar. 2010 [Revised Apr. 2012] Available: http://www.analog.com/en/products/power-management/linear-

regulators/adp151.html.

[12] Texas Instruments, "AFE4490 Integrated Analog Front End for Pulse Oximeters," AFE4490 datasheet, Dec. 2012. [Revised Jun. 2014] Available: http://www.ti.com/product/AFE4490.

[13] Linear Technology, "Dual 500mA/500mA Low Dropout, Low Noise, Micropower Linear Regulator," LT3029 datasheet, Mar. 2011[Revised Apr. 2014]. Available: http://www.linear.com/product/LT3029.

[14] STMicroelectronics, "iNEMO inertial module: 3D accelerometer, 3D gyroscope, 3D magnetometer," LSM9DS0 datasheet, Jun. 2013[Revised Aug. 2013]. Available: http://www.st.com/en/mems-and-sensors/lsm9ds0.html.

[15] Microchip, "Miniature Single-Cell, Fully Integrated Li-Ion, Li-Polymer Charge Management Controllers," MCP73831 datasheet, Nov 2005[Revised Jul. 2014]. Available: http://www.microchip.com/wwwproducts/en/en024903.

[16] Future Technology Devices International, "USB to BASIC UART IC," FT230X datasheet, Feb. 2012. [Revised May. 2016]. Available: http://www.ftdichip.com/Products/ICs/FT230X.html.

[17] Covidien, Nellcor™ with OxiMax™ Technology Product Ordering Guide, Boulder, CO: Covidien, 2011. Available: http://www.covidien.com/imageServer.aspx/doc229982.pdf?contentID=30898&contenttype=application/pdf .

[18] Agilent Technologies, "PageWriter 200/300pi User's Guide," M1771A M1770A, 1999. Available: https://isurplus.com.au/manuals/HP%20Pagewriter%20200%20ECG%20User%20Manual.pdf .

[19] Enrique Company-Bosch, Eckart Hartmann, "ECG Front-End Design is Simplified with MicroConverter," Analog Devices, Inc., 1 11 2003. [Online]. Available: http://www.analog.com/en/analog-dialogue/articles/ecg-front-end-design-simplified.html. [Accessed 6 2 2016].

[20] Kejia Li and Steve Warren, "A Wireless Reflectance Pulse Oximeter Suitable for Wearable and Surface-Integratable Designs that Produces High-Quality Unfiltered Photopethysmograms," *IEEE Transsactions on Biomedical Circuits and Systems*, vol. VI, no. 3, pp. 269-278, June 2012.

Appendix A - Hardware Schematics

Electrocardiograph

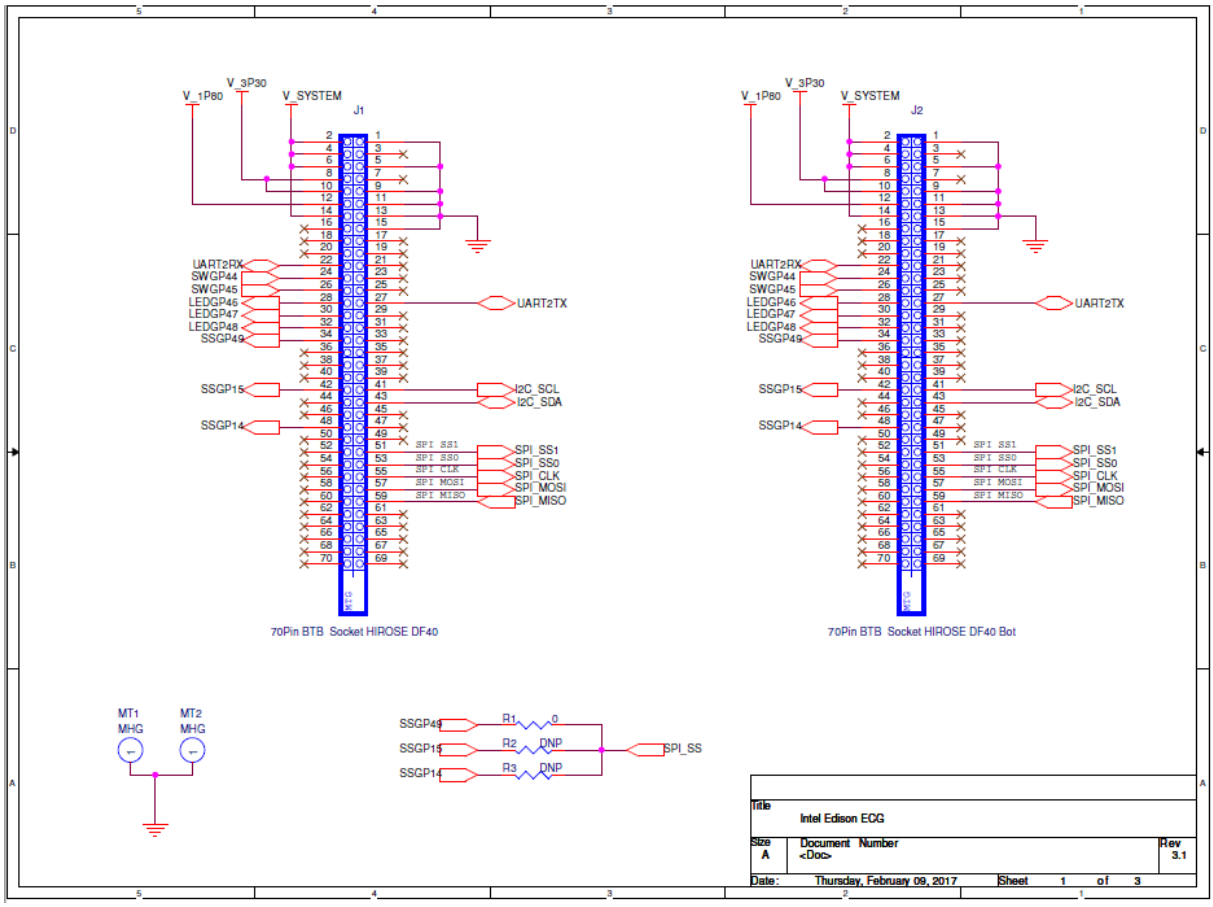

Figure 37. ECG schematics – page 1.

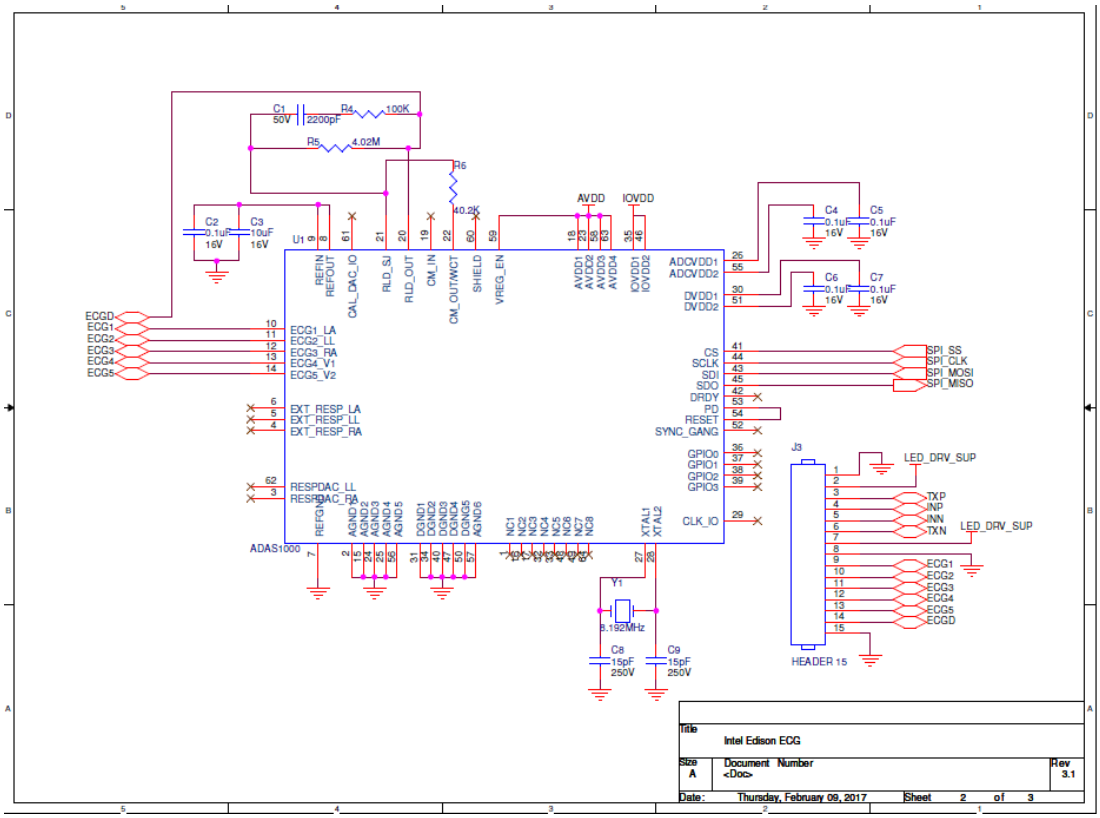

Figure 38. ECG schematics – page 2.

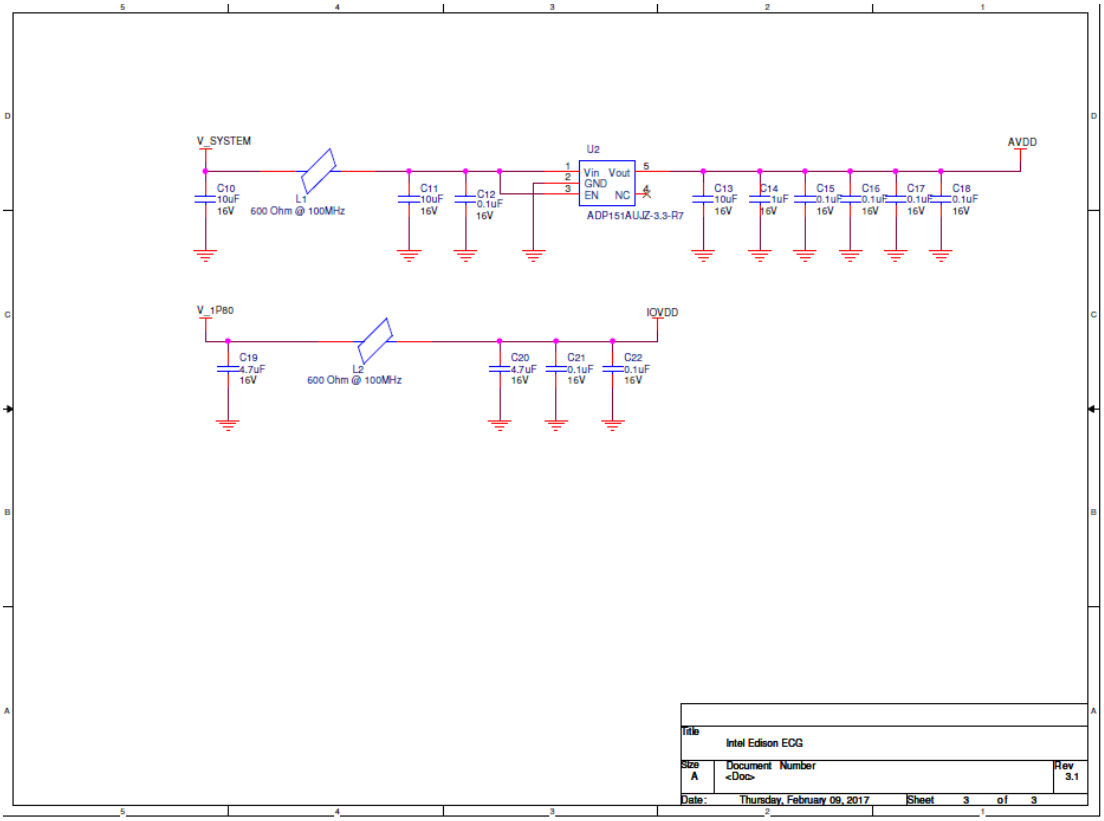

Figure 39. ECG schematics – page 3.

Pulse Oximeter

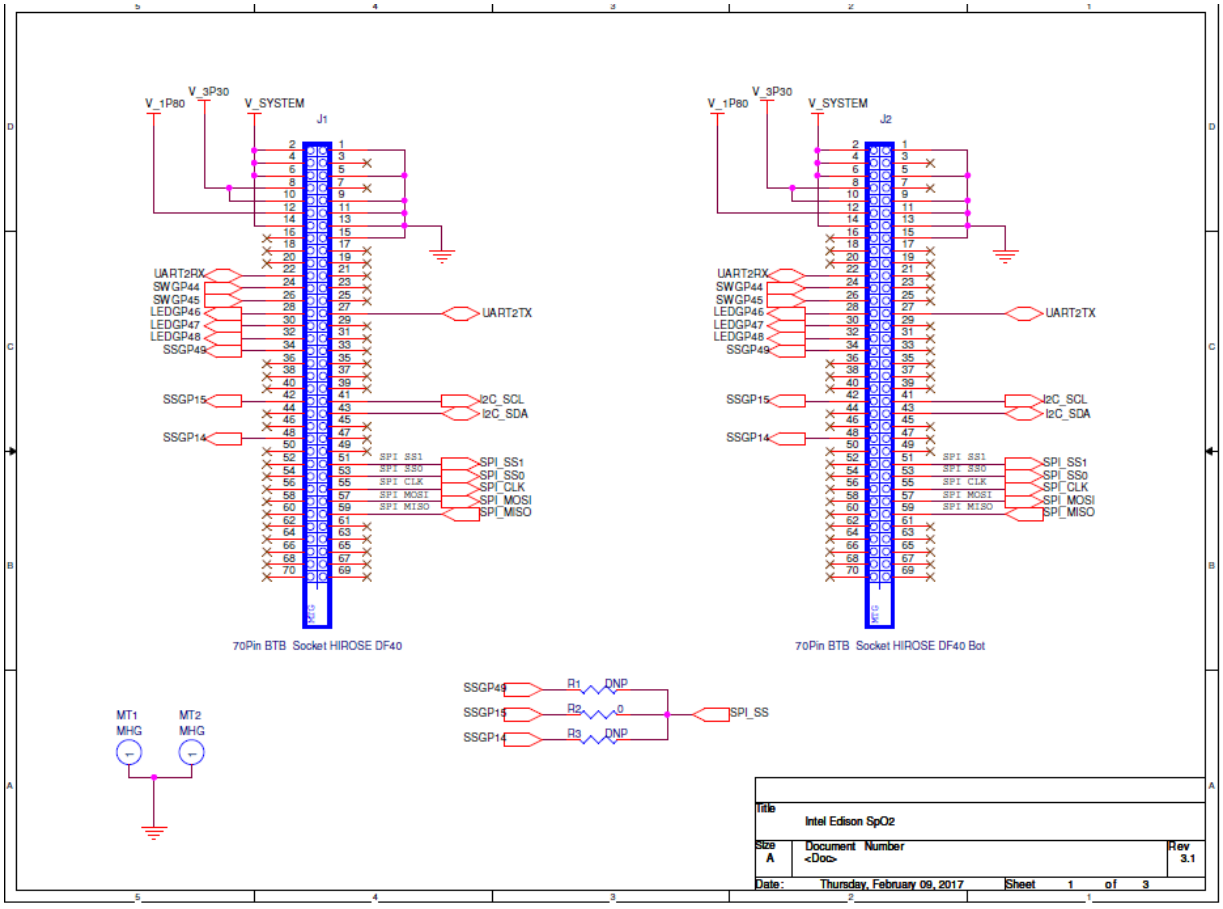

Figure 39. Pulse oximeter schematics – page 1.

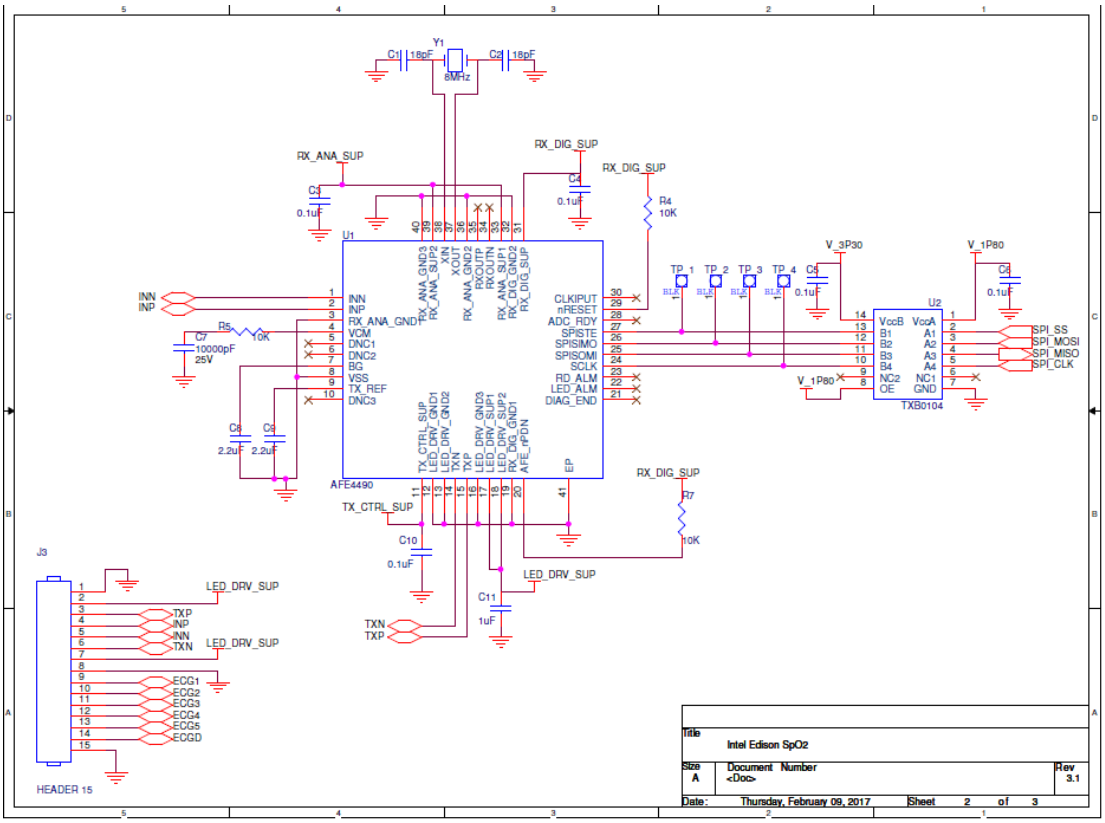

Figure 40. Pulse oximeter schematics – page 2.

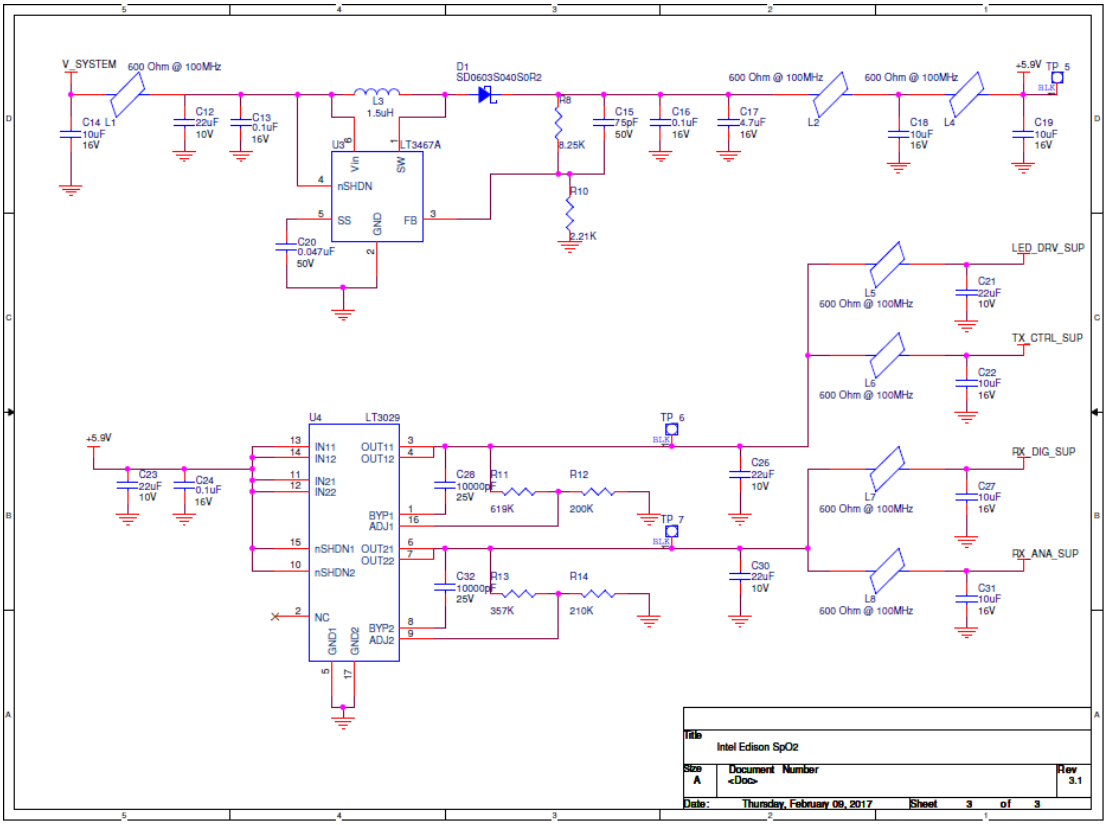

Figure 41. Pulse oximeter schematics – page 3.

Accelerometer and Gyroscope

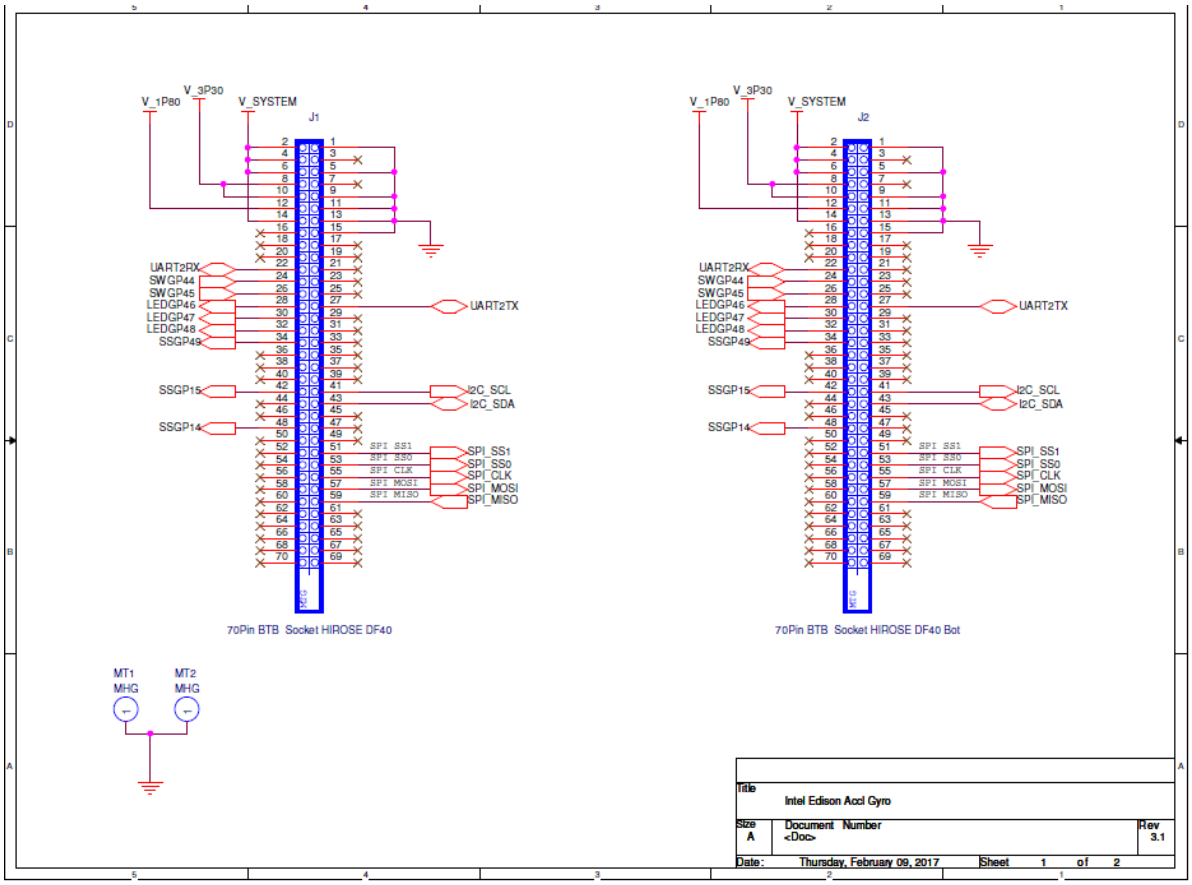

Figure 42. Accelerometer and gyroscope schematics – page 1.

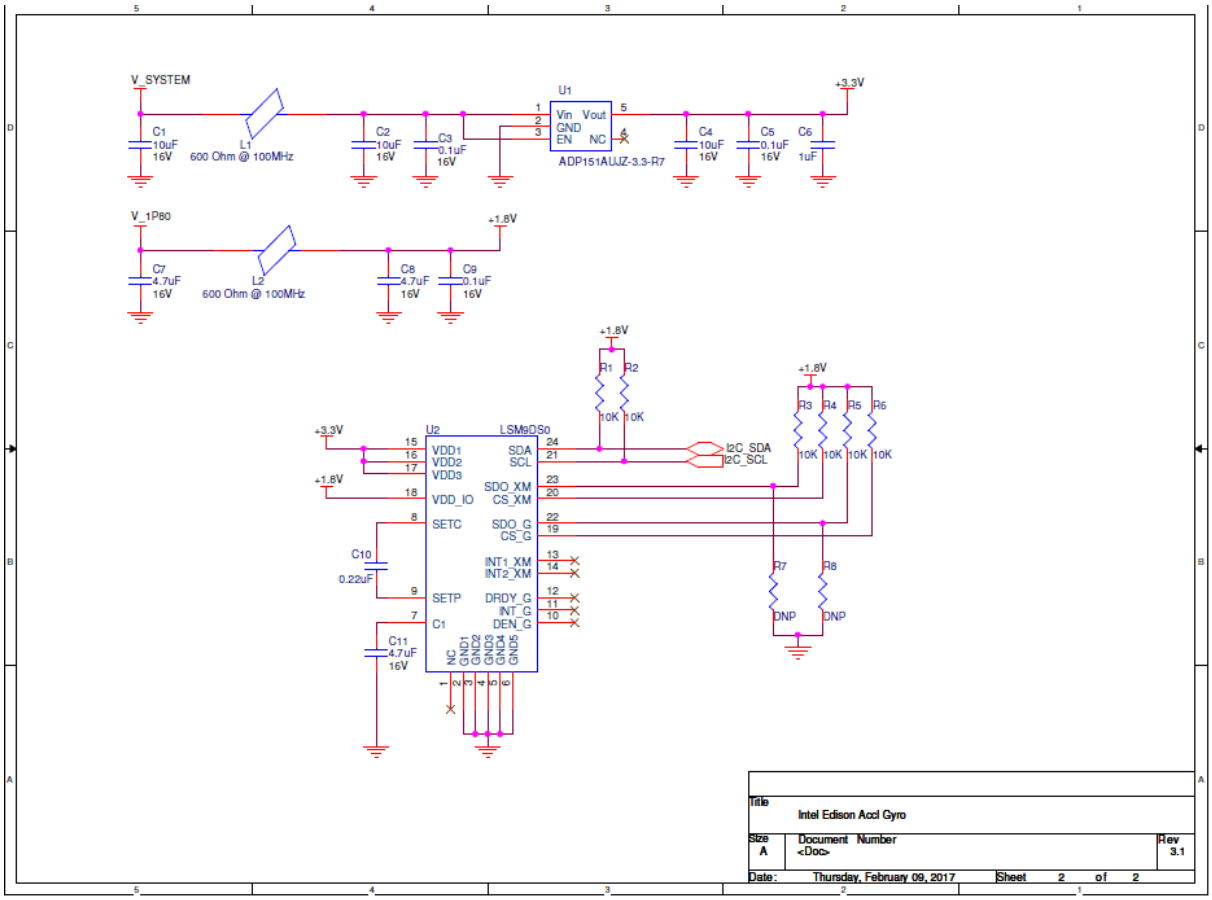

Figure 43. Accelerometer and gyroscope schematics – page 2.

Battery and Serial Port Board

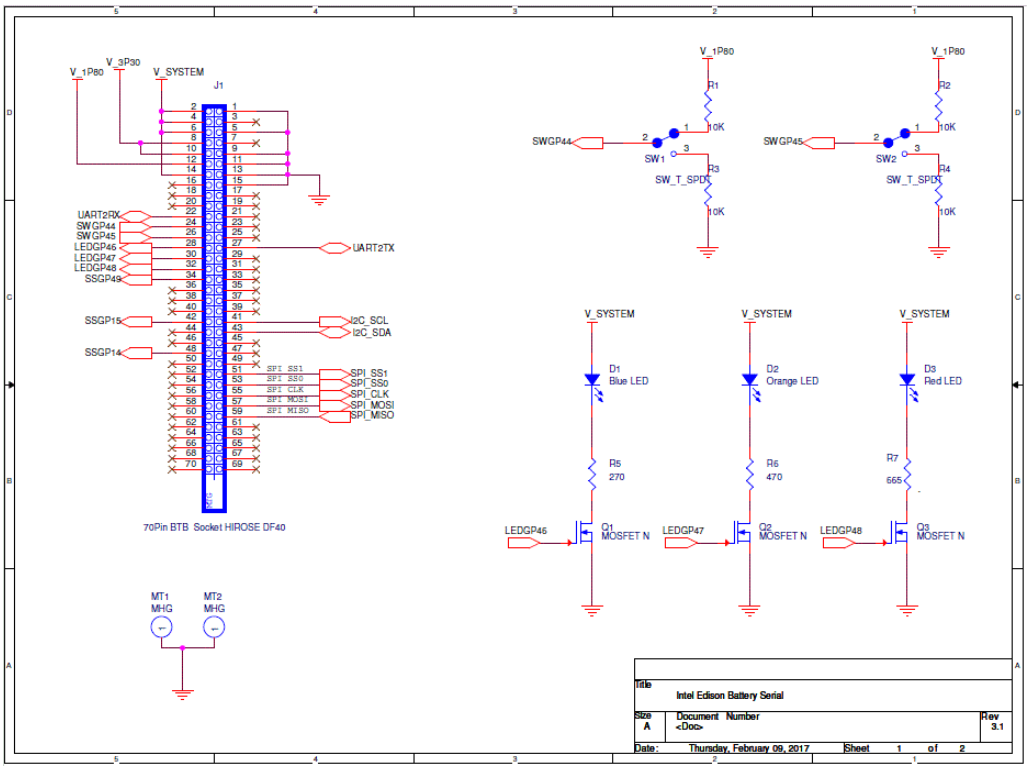

Figure 44. Battery and serial port schematics – page 1.

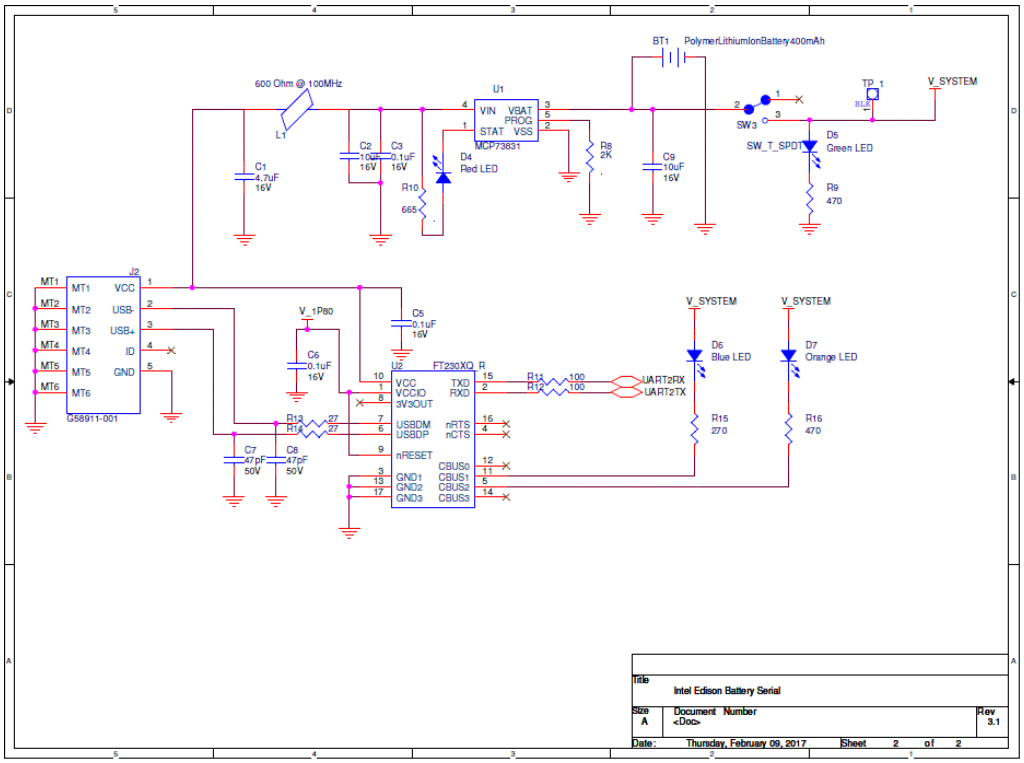

Figure 45. Battery and serial port schematics – page 2.

Appendix B - Hardware PCBs

Electrocardiograph

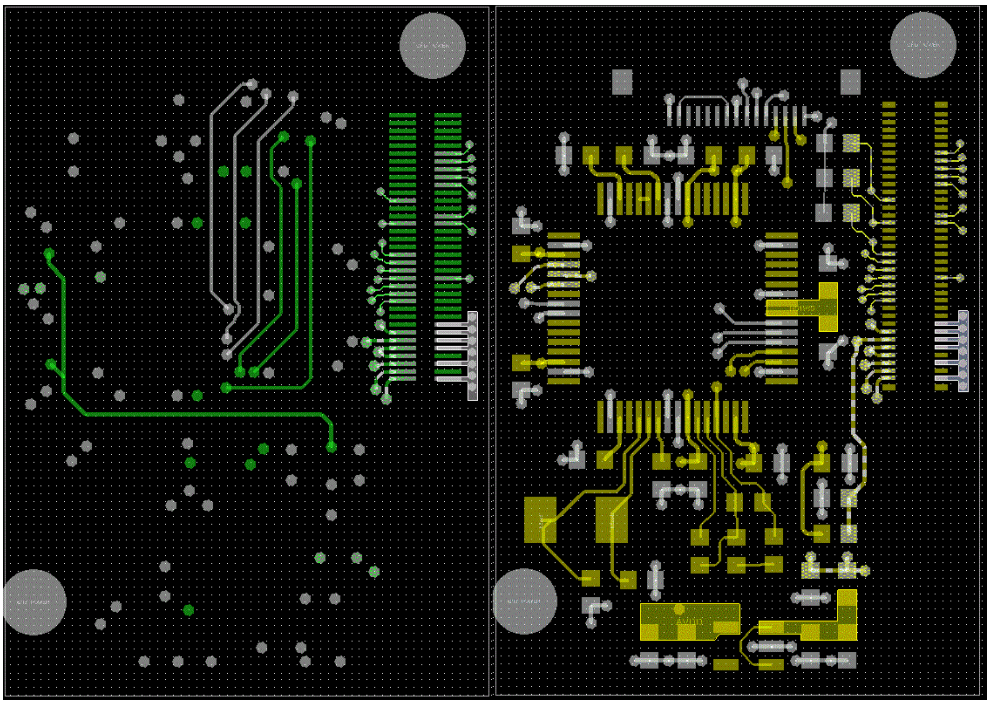

Figure 46. ECG PCB layer top and bottom.

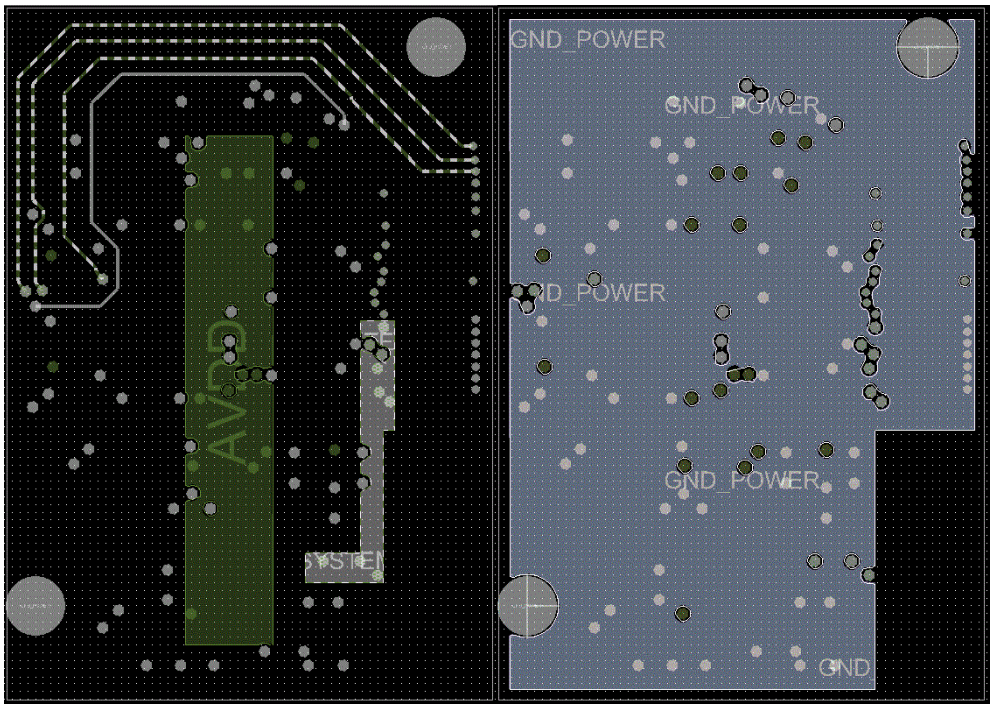

Figure 47. ECG PCB layer power and ground.

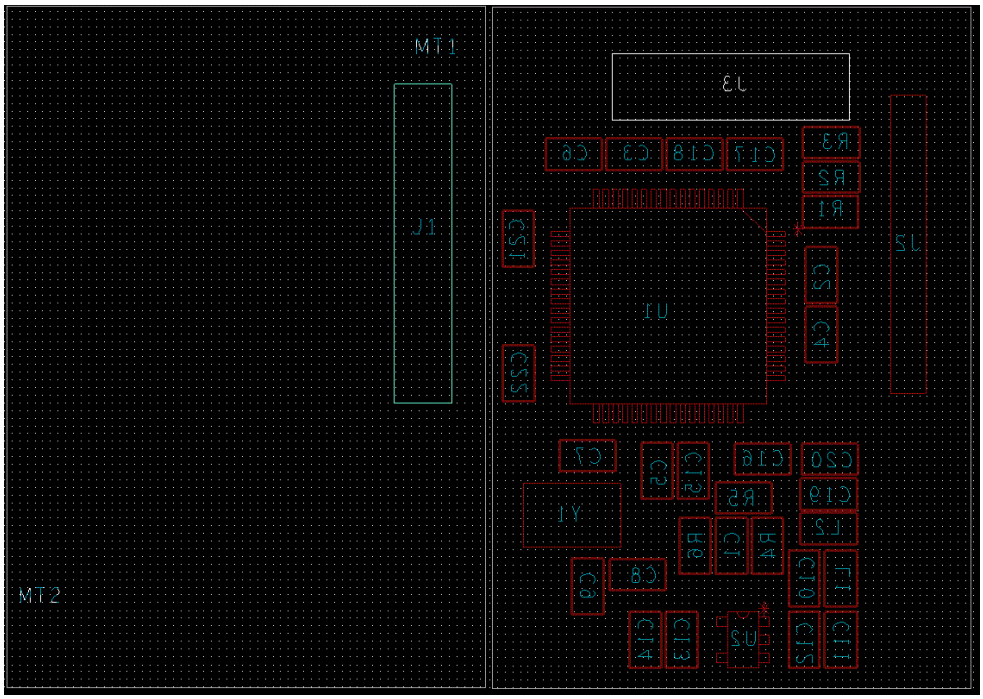

Figure 49. ECG PCB assembly top and bottom.

Pulse Oximeter

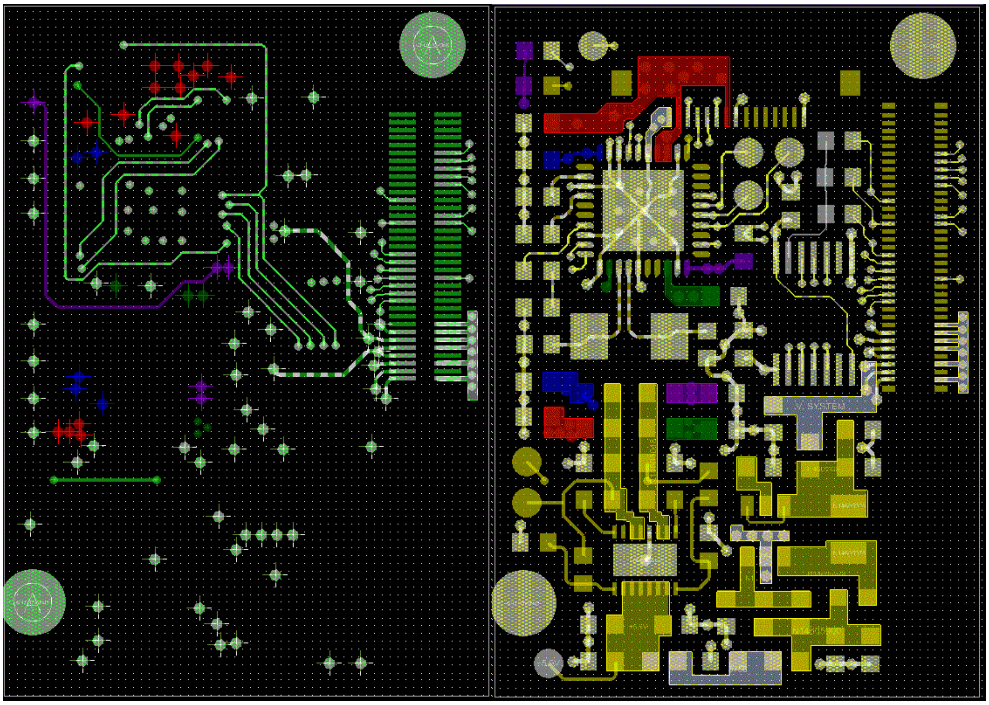

Figure 48. Pulse Oximetry PCB Layer Top and Bottom

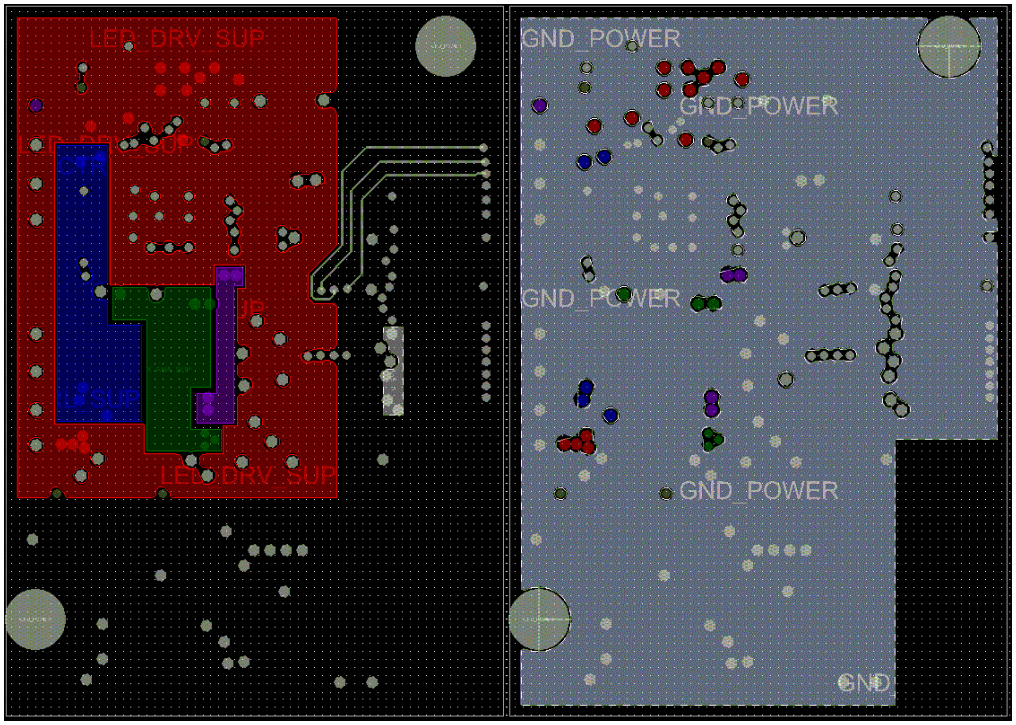

Figure 49. Pulse oximeter PCB layer power and ground.

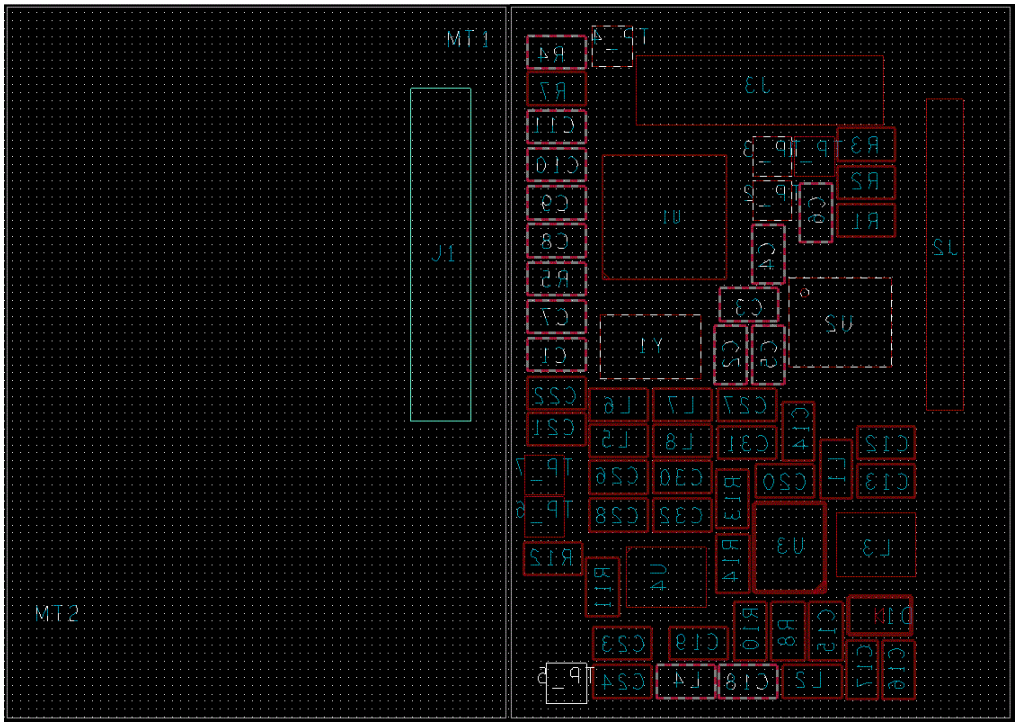

Figure 50. Pulse oximeter PCB assembly top and bottom.

Accelerometer and Gyroscope

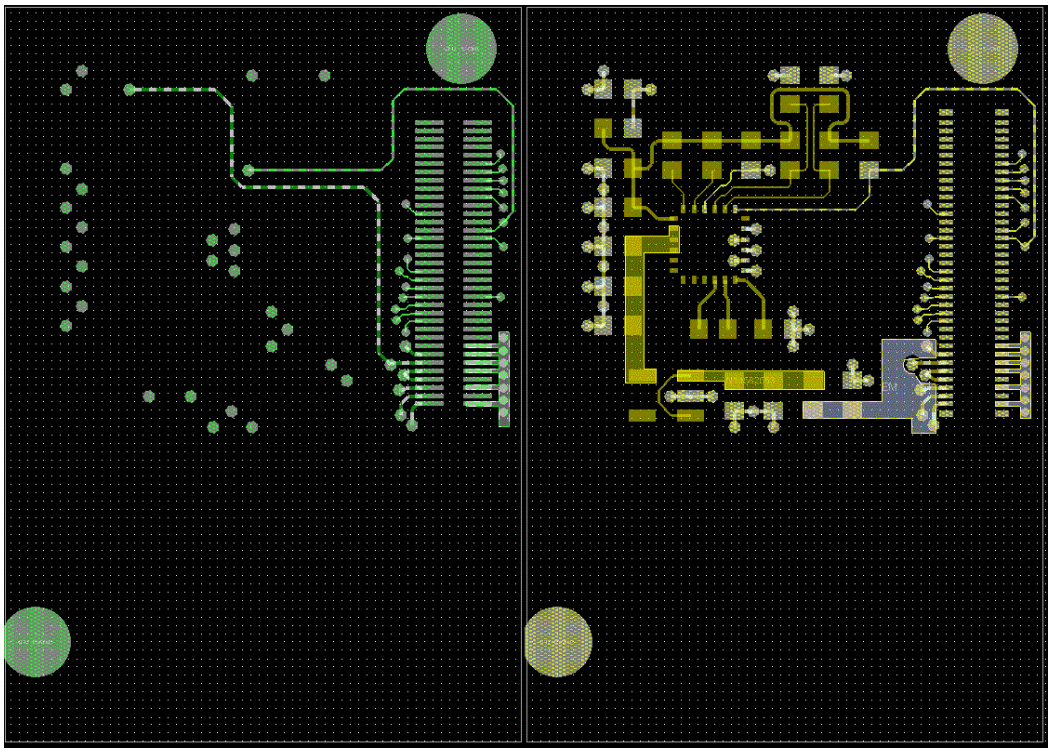

Figure 51. Accelerometer and gyroscope PCB layer top and bottom.

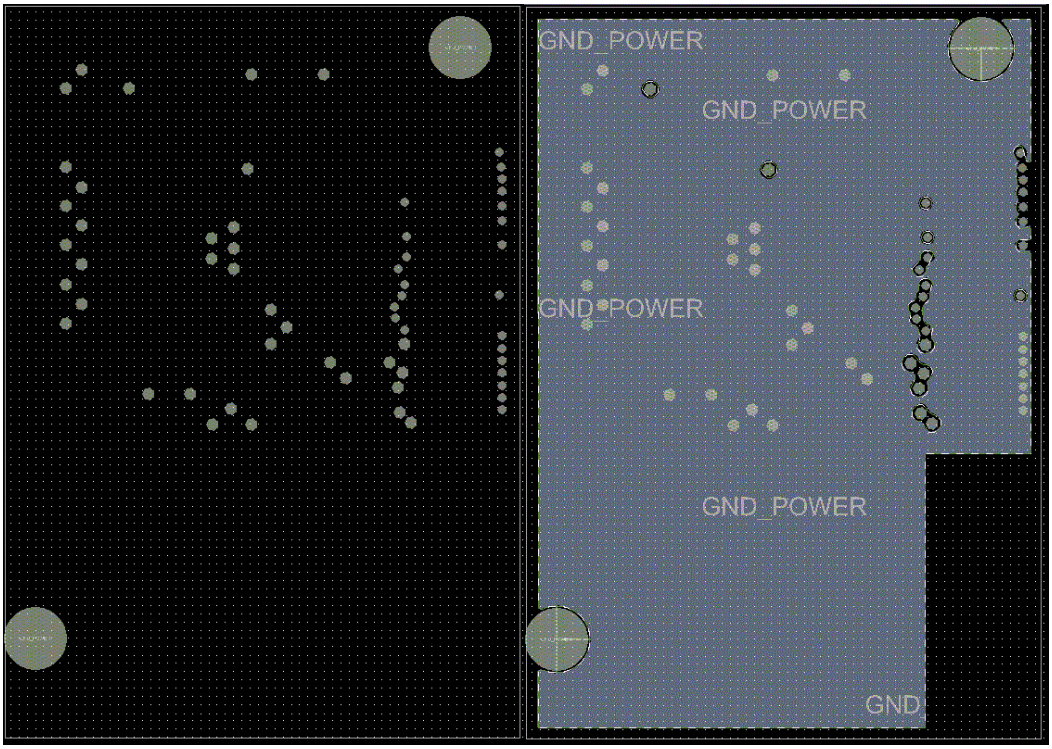

Figure 52. Accelerometer and gyroscope PCB layer power and ground.

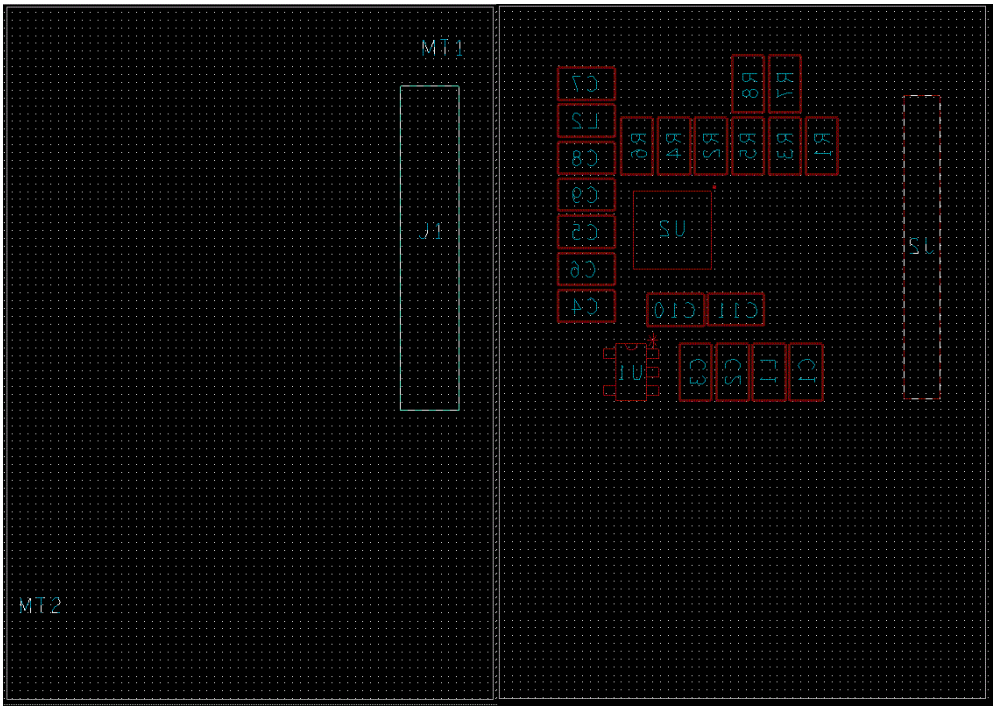

Figure 53. Accelerometer and gyroscope PCB assembly top and bottom.

Battery and Serial Port Board

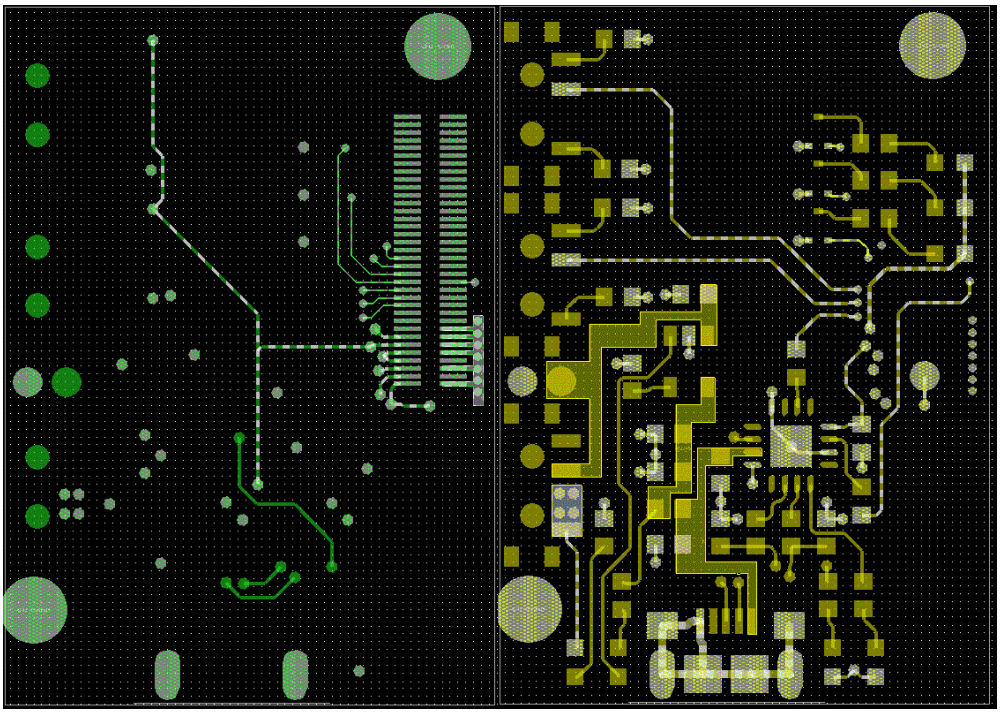

Figure 54. Battery and serial Pprt PCB layer top and bottom.

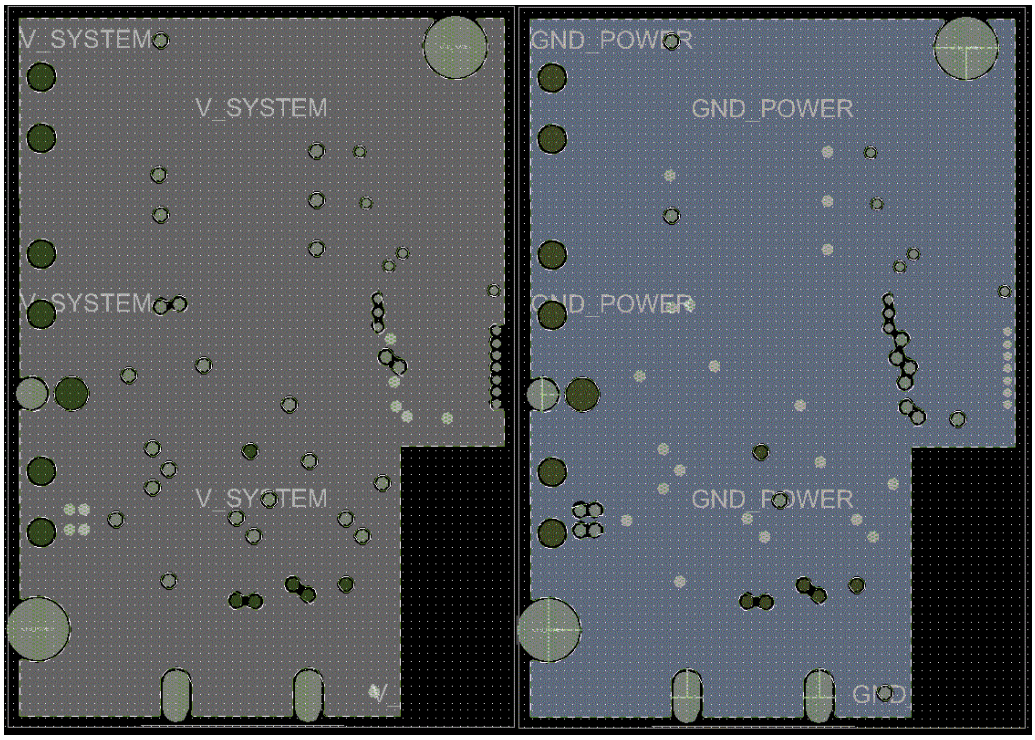

Figure 55. Battery and serial port PCB layer power and ground.

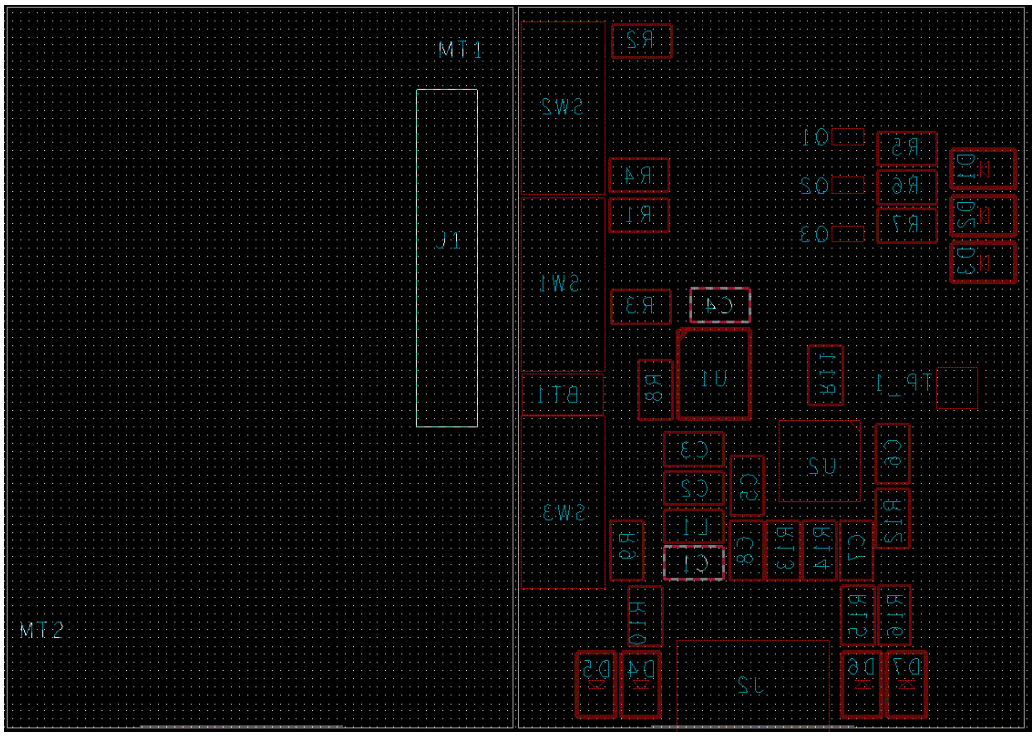

Figure 56 Battery and serial port PCB assembly top and bottom.

Appendix C - Hardware Parts Lists

Electrocardiograph

Table 3 ECG Sensor Parts List

Item	Quantity	Reference	Part	Distributor	Distributor Part no
1	1	C1	2200pF	Digi-Key	490-1459-1-ND
2	12	C2,C3,C5,C6,C7,C12,C15,	0.1uF	Digi-Key	490-9653-1-ND
		C16,C17,C18,C21,C22			
3	1	C4	10uF	Digi-Key	490-1459-1-ND
4	2	C8,C9	15pF	Digi-Key	712-1318-1-ND
5	3	C10,C11,C13	10uF	Digi-Key	445-9065-1-ND
6	1	C14	1uF	Digi-Key	445-5156-1-ND
7	2	C19,C20	4.7uF	Digi-Key	445-7478-1-ND
8	1	J1	70Pin BTB Socket HIROSE DF40	Digi-Key	H11908CT-ND
9	1	J2	70Pin BTB Plug HIROSE DF40	Digi-Key	H11630CT-ND
10	1	J3	HEADER 15	Digi-Key	OR758CT-ND
11	2	L1,L2	600 Ohm @ 100MHz	Digi-Key	490-5258-1-ND
12	2	MT1,MT2	MHG	NA	NA
13	1	R1	0	Digi-Key	311-0.0GRCT-ND
14	2	R2,R3	DNP	NA	NA
15	1	R4	100K	Digi-Key	311-0.0GRCT-ND
16	1	R5	4.02M	Digi-Key	541-4.02MHCT-ND
17	1	R6	40.2K	Digi-Key	311-40.2KHRCT-ND
18	1	U1	ADAS1000	Digi-Key	ADAS1000BSTZ-ND
19	1	U2	ADP151AUJZ-3.3-R7	Digi-Key	ADP151AUJZ-3.3-R7CT-ND
20	1	Y1	8.192MHz	Digi-Key	887-1668-1-ND

Pulse Oximeter

Table 4 Pulse Oximetry (SpO2) Sensor Parts List

Item	Quantity	Reference	Part	Distributo	Distributor Part no
1	2	C1,C2	18pF	Digi-Key	445-1272-1-ND
2	8	C3,C4,C5,C6,C10,C13,C16,	0.1uF	Digi-Key	490-9653-1-ND
		C24			
3	3	C7,C28,C32	10000pF	Digi-Key	445-2664-1-ND
4	2	C8,C9	2.2uF	Digi-Key	445-5964-1-ND
5	1	C11	1uF	Digi-Key	445-5156-1-ND
6	5	C12,C21,C23,C26,C30	22uF	Digi-Key	445-9077-1-ND
7	6	C14,C18,C19,C22,C27,C31	10uF	Digi-Key	445-9065-1-ND
8	1	C15	75pF	Digi-Key	490-1424-1-ND
9	1	C17	4.7uF	Digi-Key	445-7478-1-ND
10	1	C20	0.047uF	Digi-Key	445-14156-1-ND
11	1	D1	SD0603S040S0R2	Digi-Key	478-7798-1-ND
12	1	J1	70Pin BTB Socket HIROSE DF40	Digi-Key	H11908CT-ND
13	1	J2	70Pin BTB Plug HIROSE DF40	Digi-Key	H11630CT-ND
14	1	J3	HEADER 15	Digi-Key	OR758CT-ND
15	7	L1,L2,L4,L5,L6,L7,L8	600 Ohm @ 100MHz	Digi-Key	490-5258-1-ND
16	1	L3	1.5uH	Digi-Key	445-17123-1-ND
17	2	MT1,MT2	MHG	NA	NA
18	2	R1,R3	DNP	NA	NA
19	1	R2	0	Digi-Key	311-0.0GRCT-ND
20	3	R4,R5,R7	10K	Digi-Key	311-10.0KHRCT-ND
21	1	R8	8.25K	Digi-Key	311-8.25KHRCT-ND
22	1	R10	2.21K	Digi-Key	311-2.21KHRCT-ND
23	1	R11	619K	Digi-Key	311-619KHRCT-ND
24	1	R12	200K	Digi-Key	311-200KHRCT-ND
25	1	R13	357K	Digi-Key	311-357KHRCT-ND
26	1	R14	210K	Digi-Key	311-210KHRCT-ND
27	7	TP_1,TP_2,TP_3,TP_4,TP_5	TP_BLK	NA	NA
		TP_6,TP_7			
28	1	U1	AFE4490	Digi-Key	296-35685-1-ND
29	1	U2	TXB0104	Digi-Key	296-21929-1-ND
30	1	U3	LT3467A	Digi-Key	LT3467AES6#TRMPBFCT-ND
31	1	U4	LT3029	Digi-Key	LT3029EDE#PBF-ND
32	1	Y1	8MHz	Digi-Key	535-10630-1-ND

Accelerometer and Gyroscope

Table 5 Accelerometer and Gyroscope Sensor Parts List

Item	Quantity	Reference	Part	Distributo	Distributor Part no
1	3	C1,C2,C4	10uF	Digi-Key	445-9065-1-ND
2	3	C3,C5,C9	0.1uF	Digi-Key	490-9653-1-ND
3	1	C6	1uF	Digi-Key	445-5156-1-ND
4	3	C7,C8,C11	4.7uF	Digi-Key	445-7478-1-ND
5	1	C10	0.22uF	Digi-Key	490-11500-1-ND
6	1	J1	70Pin BTB Socket HIROSE DF40	Digi-Key	H11908CT-ND
7	1	J2	70Pin BTB Plug HIROSE DF40	Digi-Key	H11630CT-ND
8	2	L1,L2	600 Ohm @ 100MHz	Digi-Key	490-5258-1-ND
9	2	MT1,MT2	MHG	NA	NA
10	6	R1,R2,R3,R4,R5,R6	10K	Digi-Key	311-10.0KHRCT-ND
11	2	R7,R8	DNP	NA	NA
12	1	U1	ADP151AUJZ-3.3-R7	Digi-Key	ADP151AUJZ-3.3-R7CT-ND
13	1	U2	LSM9DS0	Digi-Key	497-13902-1-ND

Battery and Serial Port Board

Table 6 Battery and Serial Port Board Parts List

Item	Quantity	Reference	Part	Distributor	Distributor Part no
1	1	BT1	PolymerLithium	sparkfun	10718
2	1	C1	4.7uF	Digi-Key	445-7478-1-ND
3	2	C2,C9	10uF	Digi-Key	445-9065-1-ND
4	3	C3,C5,C6	0.1uF	Digi-Key	490-9653-1-ND
5	2	C7,C8	47pF	Digi-Key	490-1424-1-ND
6	2	D1,D6	Blue LED	Digi-Key	LNJ937W8CRACT-ND
7	2	D2,D7	Orange LED	Digi-Key	LNJ837W83RACT-ND
8	2	D3,D4	Red LED	Digi-Key	LNJ237W82RACT-ND
9	1	D5	Green LED	Digi-Key	P13485CT-ND
10	1	J1	70Pin BTB Sock	Digi-Key	H11908CT-ND
11	1	J2	G58911-001	Digi-Key	609-4616-1-ND
12	1	L1	600 Ohm @ 100	Digi-Key	490-5258-1-ND
13	2	MT1,MT2	MHG	NA	NA
14	3	Q1,Q2,Q3	MOSFET N	Digi-Key	RUE003N02TLCT-ND
15	4	R1,R2,R3,R4	10K	Digi-Key	311-10.0KHRCT-ND
16	2	R5,R15	270	Digi-Key	311-270HRCT-ND
17	3	R6,R9,R16	470	Digi-Key	311-470HRCT-ND
18	2	R7,R10	665	Digi-Key	311-665HRCT-ND
19	1	R8	2K	Digi-Key	311-2.00KHRCT-ND
20	2	R11,R12	100	Digi-Key	311-100HRCT-ND
21	2	R13,R14	27	Digi-Key	311-27.0HRCT-ND
22	3	SW1,SW2,SW3	SW_T_SPDT	Digi-Key	401-2005-1-ND
23	1	TP_1	TP_BLK	NA	NA
24	1	U1	MCP73831	Digi-Key	MCP73831T-2ATI/OTCT-ND
25	1	U2	FT230XQ_R	Digi-Key	768-1130-1-ND